



The University of Manchester

Do Dopaminergic Genes Modulate Processing Speed in Cognitive Aging? A Longitudinal Candidate Gene Study

A dissertation submitted to The University of Manchester for the degree of MSc Health Data Science in the Faculty of Biology, Medicine and Health.

Year of Submission: 2025

Student ID: 14150856

Candidate's School: Faculty of Biology, Medicine and Health

Table Of Contents

Do Dopaminergic Genes Modulate Processing Speed in Cognitive Aging? A Longitudinal Candidate Gene Study.....	1
Table Of Contents.....	2
Abstract.....	4
Declaration.....	5
Intellectual Property Statement.....	5
1. Introduction.....	6
1.1 Processing Speed Decline: A Central Feature of Cognitive Aging.....	6
1.2 Processing Speed Decline Across the Lifespan: Evidence from Longitudinal Studies.....	6
1.3 Real-World Impact and Clinical Implications.....	8
1.4 The Dopamine System and the Correlative Triad of Aging.....	8
1.5 Brain Pathology in Aging: A Potential Dopaminergic Contribution.....	10
1.6 Selecting Candidate Genes in the Dopamine Pathway.....	11
1.7 Study Rationale.....	14
2. Aims & Hypotheses.....	15
2.1 Primary Aim and Hypothesis.....	15
2.2 Secondary Aims and Hypotheses.....	15
2.3 Exploratory Aims.....	16
3. Methods.....	16
3.1 Study Cohort and Sample Selection.....	16
3.2 Genetic Data: Selection, Quality Control, and Preparation.....	16
3.3 Cognitive Battery and Domain Assessment.....	17
3.4 Cognitive Trajectory Modeling and Outcome Definition.....	18
3.5 Covariates.....	18
3.5.1 Core Covariates.....	18
3.5.2 Clinical Covariates.....	18
3.5.3 Lifestyle and Sleep Covariates.....	19
3.5.4 Additional Ancestry Principal Components.....	19
3.5.5 DAG-Based Covariate Selection.....	20
3.6 Missing Data Handling.....	20
3.7 Genetic Association Analyses.....	21
3.7.1 Single SNP Association Analysis.....	21
3.7.2 Gene-Based and Pathway-Level Analyses.....	23
3.7.3 Exploratory Pathway Component Analysis: Genetic Associations with	

Neuropathology and Synaptic Density.....	24
4. Results.....	27
4.1 Exploratory Data Analysis.....	27
4.1.1 Missing Data Overview.....	27
4.1.2 Participant Characteristics.....	28
4.1.3 Cognitive Trajectory Outcomes.....	29
4.2 Single SNP Associations with Cognitive Decline and Performance.....	31
4.2.1 Covariate Diagnostics and Population-Structure Adjustment.....	31
4.2.2 Statistical power to detect single-variant effects.....	32
4.2.3 Sensitivity Analysis: Full Sample with Modified Covariates.....	32
4.2.4 SNP Associations with Processing Speed Decline.....	33
4.2.5 Associations with Secondary Cognitive Domains (Slopes).....	35
4.2.6 SNP Associations with Cognitive Intercepts.....	35
4.2.7 SNP Associations with Secondary Cognitive Domains (Intercepts).....	37
4.3 Gene-Based Association Testing.....	37
4.3.1 Gene-Based Associations with Processing Speed Decline.....	37
4.3.2 Gene-Based Associations with Secondary Cognitive Domains (Slopes).....	38
4.3.3 Gene-Based Associations with Processing Speed Intercepts.....	38
4.3.4 Gene-Based Associations with Secondary Cognitive Domains (Intercepts).....	39
4.4 Dopamine Polygenic Risk Score Analysis.....	40
4.4.1 Statistical Power for Polygenic Score Detection.....	40
4.4.2 Dopamine Polygenic Risk Score Associations with Cognitive Decline Rates and Intercepts.....	41
4.5 Exploratory Pathway Component Analysis.....	41
4.5.1 Component 1: Genetic Associations with Neuropathology.....	41
5. Discussion.....	46
5.1 Reconciling Null Genetic Findings with Dopamine Neurobiology.....	46
5.2 Interpretation of Null Genetic Findings.....	48
5.3 Future Directions.....	50
6. Conclusion.....	51
7. References.....	53
8. Appendices.....	64

Word Count: 9912 Words

Abstract

While neuroimaging links dopamine system integrity to cognitive performance in aging, the genetic basis remains unclear. This study tested whether common dopaminergic variants influence processing speed decline, our primary outcome for its central role in cognitive aging and established dopaminergic links. We analyzed 957 variants across nine key dopamine pathway genes (synthesis: TH, DDC; receptors: DRD1-3; clearance/metabolism: SLC6A3, COMT, DBH; signal integration: PPP1R1B) in 434 participants from the University of Manchester Longitudinal Study of Cognition in Normal Healthy Old Age, examining 12-year decline rates and performance at age 70.

Across single-variant, gene-based, and polygenic risk score analyses, no associations survived multiple testing correction (Bonferroni $p < 5.22 \times 10^{-5}$). For processing speed decline rates, the strongest nominal signals were from DRD2 (gene-based $p=0.222$) and a DBH variant (rs3025383, $p=0.008$). For performance at age 70, COMT had the strongest gene-level signal ($p=0.075$), while the polygenic score was unassociated with decline ($p=0.257$). These null findings persisted across secondary cognitive domains (fluid reasoning, episodic memory, vocabulary) and in severely underpowered post-mortem analyses (neuropathology $n=116$; synaptic density $n=50$).

Crucially, with 80% power to detect single variants explaining $\geq 5.3\%$ variance ($\beta \geq 0.24$ SD) and polygenic effects of $|\beta| \geq 0.14$, the absence of detectable effects above these thresholds provides evidence against genetic effects of this magnitude, though smaller effects cannot be excluded.

These findings suggest the disconnect between neurobiology and genetics arises from complex mechanisms not captured by common variant analysis, such as rare variants, epigenetic regulation, or gene-environment interactions. This supports a highly polygenic model of cognitive aging that requires larger samples to detect thousands of variants with minute effects. This study demonstrates how well-powered null findings advance our understanding of complex trait architecture.

Declaration

No portion of the work referred to in the dissertation has been submitted in support of an application for another degree or qualification of this or any other university or other institute of learning.

Intellectual Property Statement

- i. The author of this dissertation (including any appendices and/or schedules to this dissertation) owns certain copyright or related rights in it (the "Copyright") and s/he has given The University of Manchester certain rights to use such Copyright, including for administrative purposes.
- ii. Copies of this dissertation, either in full or in extracts and whether in hard or electronic copy, may be made only in accordance with the Copyright, Designs and Patents Act 1988 (as amended) and regulations issued under it or, where appropriate, in accordance with licensing agreements which the University has entered into. This page must form part of any such copies made.
- iii. The ownership of certain Copyright, patents, designs, trademarks and other intellectual property (the "Intellectual Property") and any reproductions of copyright works in the dissertation, for example graphs and tables ("Reproductions"), which may be described in this dissertation, may not be owned by the author and may be owned by third parties. Such Intellectual Property and Reproductions cannot and must not be made available for use without the prior written permission of the owner(s) of the relevant Intellectual Property and/or Reproductions.
- iv. Further information on the conditions under which disclosure, publication and commercialisation of this dissertation, the Copyright and any Intellectual Property and/or Reproductions described in it may take place is available in the University IP Policy, in any relevant Dissertation restriction declarations deposited in the University Library, and The University Library's regulations.

1. Introduction

1.1 Processing Speed Decline: A Central Feature of Cognitive Aging

As the world's 65+ cohort is projected to reach 1.6 billion by 2050 (United Nations, 2022), understanding cognitive aging has become a pressing scientific challenge. Among the mental abilities that decline with age, processing speed is particularly fundamental. Statistically accounting for its decline reveals that it explains up to 95% of the age-related variance in reasoning and working memory and underscores cognitive slowing as a primary pathway of broader cognitive aging (Salthouse, 1991).

Processing speed, the time required for basic operations, links to higher cognition through two key mechanisms (Salthouse, 1996): the "limited time" mechanism, where slow initial processing constrains subsequent operations, and the "simultaneity" mechanism, where information decays before integration. These mechanisms imply that slower basic speed mediates much of the age effect on complex cognition, a conclusion supported by evidence that controlling for processing speed reduces age-related cognitive variance by an average of approximately 83% (Salthouse, 1996).

Unlike knowledge-based abilities, processing speed reflects neural efficiency and shows a steady, near-linear decline from early adulthood (Salthouse, 1996). This is a robust phenomenon, confirmed by a meta-analysis that found a strong and consistent correlation between age and processing speed ($r=-0.52$) (Verhaeghen & Salthouse, 1997). Such decline has significant real-world repercussions, correlating with increased fall risk and compromised driving safety (Davis et al., 2017; Anstey et al., 2005). This establishes processing speed decline as a crucial marker of functional risk, making the investigation of its underlying mechanisms essential.

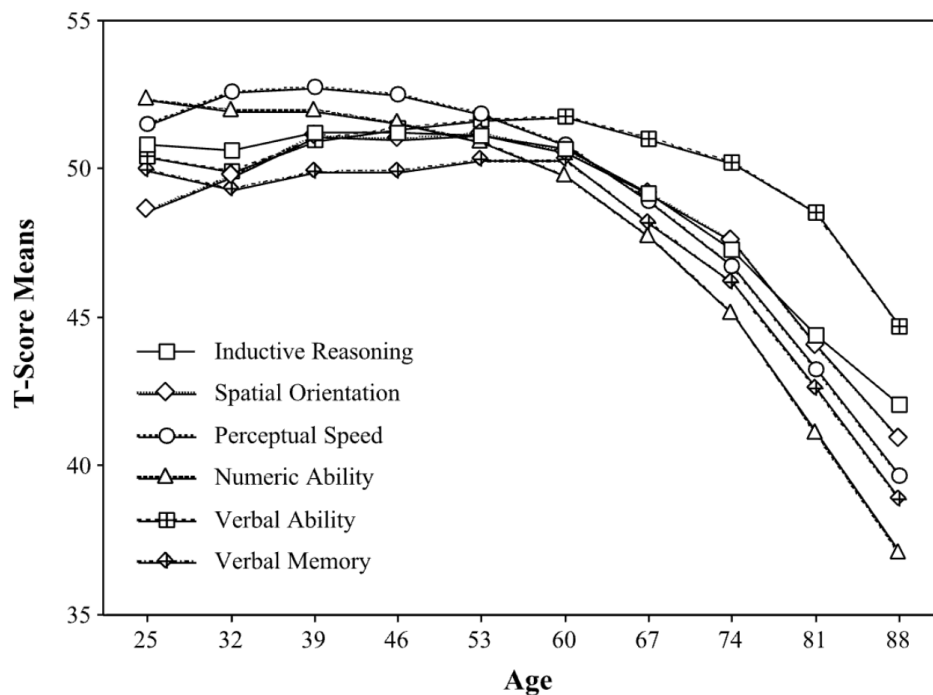
1.2 Processing Speed Decline Across the Lifespan: Evidence from Longitudinal Studies

To better understand these mechanisms and individual differences in decline trajectories, longitudinal research has tracked processing speed changes across adulthood, revealing clear group-level patterns alongside substantial individual variation. The Seattle Longitudinal Study (SLS), one of the most comprehensive sources

of evidence, has followed more than 5,000 adults in repeated waves since 1956 using rapid visual-matching tasks to measure processing speed, providing detailed data on both average cognitive change and within-person differences (Schaie et al., 2004).

As illustrated in Figure 1, the SLS data show that processing speed exhibits a substantial age-related decline that begins in midlife (around age 53) and accelerates in later decades, positioning it as a sensitive, early marker of cognitive aging (Schaie et al., 2004).

Figure 1. Age-related trajectories in six cognitive domains in the Seattle Longitudinal Study.



Mean standardized T-scores ($M=50$, $SD=10$ at age 60) for six cognitive domains across nine age bands (25–88 years). Source: Reproduced from Schaie et al. (2004).

However, not everyone follows the same trajectory. For instance, trajectory modeling of ten-year data from the English Longitudinal Study of Ageing ($N=12,099$) identified four distinct processing-speed profiles based on letter cancellation tests. Notably, one group (19.6% of participants) was characterized by a severe course of progressive decline from a low initial performance (Gkotzamanis et al., 2021). The existence of such distinct trajectories underscores the importance of identifying factors that account for individual differences in processing speed aging.

1.3 Real-World Impact and Clinical Implications

Identifying the factors driving individual differences is crucial, as processing speed decline is both modifiable and predictive of future cognitive health outcomes.

Intervention studies have demonstrated modifiability, while prospective studies link decline to dementia risk.

Intervention studies demonstrate that targeted training can reduce dementia risk. The ACTIVE (Advanced Cognitive Training for Independent and Vital Elderly) trial's ten-year follow-up of 2,802 older adults showed that computerized speed-of-processing training (Useful Field of View) lowered dementia risk by 29% ($HR = 0.71$, 95% CI 0.50–0.998), with each additional training session providing another 10% risk reduction (Edwards et al., 2017). These findings suggest that processing speed is not only modifiable but that improvements can translate into meaningful protection against dementia.

Prospective cohort studies have established processing speed decline as a predictor of future cognitive impairment. In the four-year Sydney Memory and Ageing Study of 861 adults, for example, slower performance on simple and choice reaction time tasks predicted dementia onset. Each standard-deviation increase in response time was associated with a 50–60% elevation in risk ($HR=1.53\text{--}1.59$), a finding that held after controlling for other cognitive and health factors (Kochan et al., 2016). Processing speed is therefore a sensitive marker of brain vulnerability and a modifiable target for intervention, yet its underlying biological mechanisms are unclear. Converging evidence implicates dopaminergic pathways, which are explored below.

1.4 The Dopamine System and the Correlative Triad of Aging

Bäckman et al. (2006) introduced the correlative triad, a framework describing the interrelated associations among adult age, dopamine system integrity, and cognitive performance. According to this model, age-related declines in dopaminergic function may contribute to cognitive aging, particularly in domains that rely on rapid and efficient information processing. This framework positions dopamine decline as both a potential indicator and mechanism underlying age-related cognitive change.

Defining the Correlative Triad

The first component demonstrates that dopaminergic markers decline with age. Post-mortem and neuroimaging studies show D1 and D2 receptor densities and dopamine transporter availability decrease approximately 10% per decade, with reductions extending beyond the striatum to frontal, temporal, parietal, and occipital cortices, plus hippocampus, amygdala, and thalamus, indicating widespread dopaminergic change (Bäckman et al., 2006).

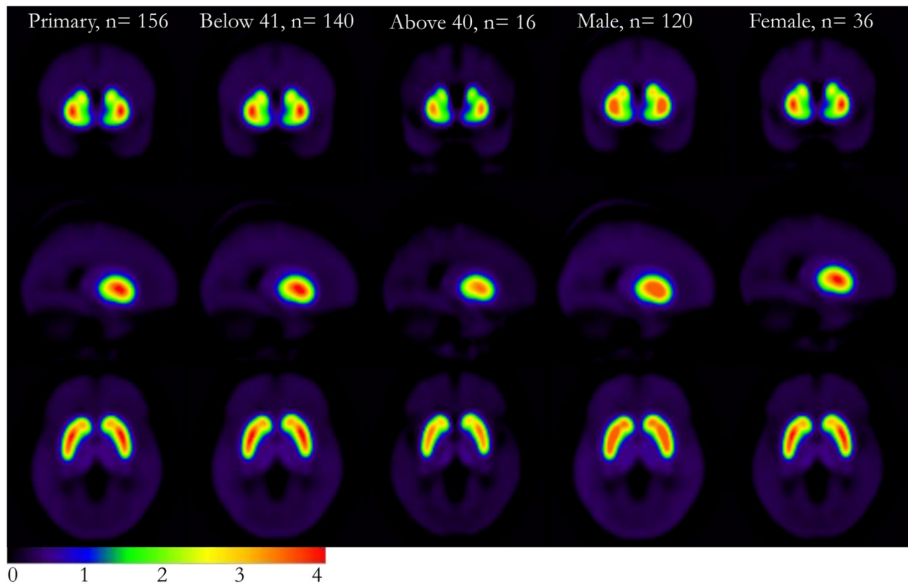
The second component shows dopamine markers predict cognitive performance across multiple domains. In a PET investigation, Bäckman et al. (2000) demonstrated that statistical control of striatal D2 receptor binding substantially reduced age-related cognitive effects, while D2 binding independently contributed to performance beyond chronological age across domains including episodic memory and perceptual speed.

The third and most crucial component reveals that dopamine decline actively mediates rather than merely correlates with age-related cognitive deficits. Statistical control of dopamine markers dramatically reduced age-related cognitive variance, with some studies showing near-complete elimination of age effects across different markers (D1, D2, DAT) and cognitive domains, establishing dopamine activity as a key constraint on cognitive performance throughout adulthood (Bäckman et al., 2006).

Quantifying Dopamine System Decline

Karrer et al.'s (2017) comprehensive meta-analysis of 95 PET and SPECT datasets ($N=2,611$) quantified dopamine system decline, providing empirical validation for the correlative triad predictions. D1 receptors exhibited the steepest age effect ($r=-0.77$), followed by dopamine transporters ($r=-0.68$) and D2 receptors ($r=-0.56$), with decline rates ranging from 3.7% to 14.0% per decade depending on marker and region. Importantly, dopamine synthesis capacity showed no reliable age trend, indicating the primary deficit involves receptor loss and reuptake efficiency rather than production. This age-related loss in receptor availability is clearly visualized in group-average PET maps from a large cohort study by Malén et al. (2022) (Figure 2). These images demonstrate that striatal D2/3 binding is markedly lower in older versus younger adults, and that females show slightly higher binding than males at each age.

Figure 2. Age and sex differences in dopamine D2/3 receptor availability.



Mean binding-potential (BPND) maps of dopamine D2/3 receptor availability in 156 healthy adults, stratified by age and sex. Warmer colors (red, yellow) denote higher receptor availability.
Source: Malén et al. (2022). Reproduced under CC BY-NC-ND 4.0 license.

Functional Significance for Processing Speed

The functional significance of dopamine decline for processing speed is supported by PET imaging, which reveals that lower striatal D2 receptor availability strongly predicts poorer performance on perceptual-speed tasks (Bäckman et al., 2000). Pharmacological studies provide causal evidence: L-DOPA selectively accelerates early stimulus-processing stages (Rihet et al., 2002), and dopamine agonists reduce task-switch costs (Cools and D'Esposito, 2011).

Longitudinal studies further strengthen this framework. For example, a five-year study of the COBRA/DyNAMiC project found that declines in striatal D2 binding predicted working-memory deterioration (Karalija et al., 2024). Given the well-established correlations between working memory and processing speed in aging, these findings suggest that dopamine decline likely affects multiple cognitive domains through shared mechanisms. Direct molecular imaging confirms this relationship: higher striatal dopamine-transporter levels correlate with faster reaction times in older adults even after controlling for age (van Dyck et al., 2008).

1.5 Brain Pathology in Aging: A Potential Dopaminergic Contribution

While the correlative triad model is powerful, it may be incomplete, as cognitive aging is also strongly associated with brain pathology, a factor linked to cognitive decline even in clinically normal older adults. For instance, greater tau burden predicts poorer cognition (Wennberg et al., 2019), and higher tau and β -amyloid levels are linked to worse memory outcomes (Marks et al., 2017).

The clinical relevance of this pathology motivates investigating whether the dopamine system contributes to cognitive aging via such indirect mechanisms. A plausible biochemical pathway is hypothesized from convergent evidence: dopamine metabolism generates chronic oxidative stress (Juárez-Olguín et al., 2016), a process implicated in cognitive aging (Kandlur et al., 2020) that also facilitates protein aggregation into pathological lesions via toxic dopamine quinones (Meiser et al., 2013). While this specific cascade has not been directly demonstrated, this synthesis provides a strong theoretical rationale for investigating whether dopaminergic genetics might influence cognitive aging indirectly, through an effect on the development of brain pathology.

1.6 Selecting Candidate Genes in the Dopamine Pathway

This study investigates the genetic basis of dopamine's role in cognitive aging, particularly its influence on processing speed, by examining nine core genes selected for comprehensive coverage of the dopamine pathway. These genes represent the full biological process, from synthesis to post-synaptic signaling, as illustrated in the functional architecture of the synapse (Figure 3).

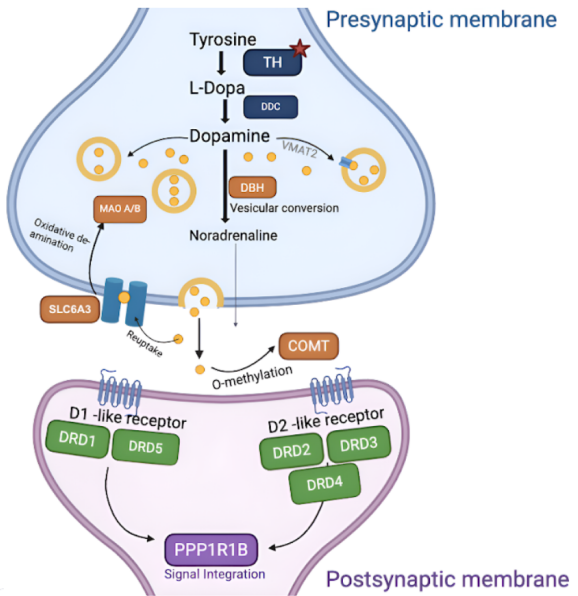
Figure 3. The Dopamine Synapse and Key Pathway Genes.

Colour-coded gene classes

- Synthesis enzymes (TH★, DDC)
- Dopamine receptors (DRD1, DRD2, DRD3, DRD4, DRD5)
- Clearance / metabolism genes (SLC6A3, DBH, COMT, MAO A/B)
- Signal integration gene (PPP1R1B)

Additional symbol

★ indicates rate-limiting step in dopamine synthesis (TH)



A schematic of the dopamine pathway, from synthesis in the presynaptic neuron to receptor binding and signal integration in the postsynaptic neuron. Adapted from Moura & Vale (2023) and Xu & Yang (2022); created with BioRender.com.

An initial panel of thirteen dopamine-pathway genes was prespecified, with four subsequently excluded during quality control: MAOA and MAOB (as X-chromosome variants were not analyzed), DRD4 (no probe coverage), and DRD5 (failed QC). The remaining nine autosomal genes provide broad coverage of the pathway, spanning synthesis (TH, DDC), receptor signaling (DRD1-3), clearance and metabolism (SLC6A3, COMT, DBH), and signal integration (PPP1R1B). The full selection procedure is detailed in the Methods (Section 3.2).

The following subsections detail each gene's role in the dopamine pathway and its established relevance to cognitive function, forming the theoretical basis for its investigation in the domain of processing speed.

Dopamine Synthesis Genes: Setting the Input Signal

Tyrosine hydroxylase (TH) catalyses the rate-limiting step in dopamine synthesis, converting tyrosine to L-DOPA. The promoter SNP rs10770141 increases TH transcription in vitro and enhances catecholamine production (Zhang et al., 2010). PET imaging shows that individuals with higher striatal dopamine synthesis capacity have faster task-switching reaction times, a key cognitive flexibility measure (Berry et al.,

2016). Since TH initiates the catecholamine pathway, functional variation within the gene is a plausible modulator of processing speed.

DOPA decarboxylase (DDC) completes synthesis by converting L-DOPA to dopamine. PET evidence links DDC allelic variation to dopamine synthesis capacity (Eisenberg et al., 2016), suggesting its genetic variation may be important for maintaining processing speed as compensatory capacity declines with age.

Dopamine Receptor Genes: Translating Dopamine into Neural Gain

Dopamine receptor D1 (DRD1) is the most abundant cortical receptor, showing the steepest age-related decline among dopaminergic markers ($\beta \approx -0.59$; Karrer et al., 2017). Lower D1 availability links to poorer cognitive performance in older adults (Rieckmann et al., 2011), suggesting genotypes reducing D1 signaling contribute to age-related slowing.

Dopamine receptor D2 (DRD2) density declines by roughly 10% per decade. Functional variants like Taq1A (rs1800497) and C957T (rs6277) alter receptor availability and predict perceptual-speed performance (Hirvonen et al., 2009), suggesting reduced D2 signaling could contribute to psychomotor decline.

Dopamine receptor D3 (DRD3) is expressed in limbic-striatal regions and contributes to flexible, reward-guided behaviour (Le Moine and Bloch, 1996). The Ser9Gly missense variant (rs6280) increases dopamine binding affinity and alters receptor signalling (Lundström and Turpin, 1996). Gly-allele carriers exhibit slower task switching and more perseverative errors on executive tasks (Lane et al., 2008), effects more pronounced in older adults (Hupfeld et al., 2018). These findings suggest DRD3 variation contributes to individual differences in speeded cognitive flexibility across adulthood.

Dopamine Clearance and Metabolism Genes: Controlling Signal Duration

The dopamine transporter (SLC6A3) controls dopamine signal duration by clearing synaptic dopamine. Its expression is modulated by a 40-bp VNTR, with the 10-repeat allele increasing striatal transporter density and affecting cognitive speed (Michelhaugh et al., 2001; Heinz et al., 2000). In normal aging, higher SLC6A3 availability correlates with slower reaction times, suggesting overly rapid clearance may be detrimental (van Dyck et al., 2008; Erixon-Lindroth et al., 2005). Conversely, in Parkinson's disease, higher transporter availability associates with faster processing speed (Vriend et al.,

2020). These convergent findings establish SLC6A3 as a key modulator of processing speed.

Catechol-O-methyltransferase (COMT) Val158Met (rs4680) alters cortical dopamine half-life by approximately 40 %. Meta-analyses associate the Val allele with slower Stroop and Trail-Making performance, in which reaction time is the principal outcome (Barnett et al., 2008). The present longitudinal design will assess whether this disadvantage amplifies over decades.

Dopamine beta-hydroxylase (DBH) converts dopamine to norepinephrine, regulating dopamine-norepinephrine balance in prefrontal circuits. The rs1611115 (C-1021T) variant produces up to 10-fold differences in enzyme activity, with reduced activity leading to higher cortical dopamine levels (Parasuraman et al., 2012). The G allele of rs1108580 associates with superior working memory performance (Parasuraman et al., 2005), while low DBH activity links to speedier decision-making under cognitive load (Parasuraman et al., 2012). DBH genetic variation represents a plausible moderator of processing speed decline during aging.

Signal-Integration Gene: Tuning Cortico-striatal Circuitry

Protein phosphatase 1 regulatory subunit 1B (PPP1R1B) encodes DARPP-32, a phosphoprotein that integrates D1-mediated excitation with D2-mediated inhibition, regulating cortico-striatal circuit gain. PPP1R1B variants associate with enhanced frontostriatal cognitive performance and increased prefrontal connectivity (Meyer-Lindenberg et al., 2007). The rs907094 variant specifically affects attentional flexibility, with A homozygotes showing greater cognitive control than G carriers (Li et al., 2013). Because DARPP-32 operates where cortical input translates into striatal output, its genetic variation may influence neural efficiency and processing speed during aging.

1.7 Study Rationale

While strong evidence links dopamine system integrity to cognitive aging, the genetic underpinnings remain poorly understood. The preceding review of candidate genes highlights that although many are linked to functions like working memory and executive control, direct evidence for their role in processing speed is sparse. However, given that age-related effects on these cognitive domains are highly shared rather than independent, it is plausible that the cumulative genetic architecture of the dopamine pathway contributes to processing speed decline.

Therefore, the present study addresses this gap with a targeted, pathway-level approach. We will primarily test for direct genetic associations with the 12-year rate of processing speed decline in an aging cohort, while also exploring potential indirect mechanisms linking these genes to underlying neuropathology.

2. Aims & Hypotheses

2.1 Primary Aim and Hypothesis

Aim: Examine associations between common variants in nine dopamine pathway genes and processing speed decline rates (slopes) over 12 years as the primary cognitive outcome.

Hypothesis: Common variants in dopamine pathway genes will be significantly associated with individual differences in processing speed decline rates, given the well-established connections between dopamine system integrity and processing speed performance in aging.

2.2 Secondary Aims and Hypotheses

Aim 1: Examine associations between dopamine pathway genetic variants and processing speed performance at age 70 (intercepts) as a secondary analysis to complement the primary slopes analysis.

Hypothesis: Dopaminergic genetic variants will be associated with processing speed performance levels in addition to decline rates.

Aim 2: Examine associations between dopamine pathway genetic variants and decline trajectories in secondary cognitive domains (fluid reasoning, episodic memory, vocabulary slopes and intercepts) to assess domain-specificity of dopaminergic genetic effects.

Hypothesis: Effects will be detectable across cognitive domains but strongest for processing speed given its established neurobiological links to dopamine function compared to other cognitive abilities.

Aim 3: Investigate gene-based and pathway-level effects using MAGMA gene-based testing and construct a dopamine polygenic risk score (dPRS) to capture cumulative genetic effects across the dopamine pathway.

Hypothesis: Gene-based tests and polygenic risk scores will detect pathway-level effects missed by single-SNP analyses, particularly for the primary processing speed decline outcome.

2.3 Exploratory Aims

Aim 4: Conduct exploratory pathway component analysis using post-mortem brain tissue data (n=116 neuropathology, n=50 synaptic density) to investigate potential neurobiological mechanisms underlying genetic effects on cognitive aging.

Component 1: Test associations between dopamine pathway variants and neuropathological markers (Braak stage, Thal phase, cerebral amyloid angiopathy, α -synuclein, TDP-43) and synaptic density measures.

Component 2: Examine associations between brain pathology markers and cognitive trajectories, focusing on processing speed decline.

Hypothesis: Dopaminergic genetic variants may influence cognitive aging through effects on brain pathology, which should predict cognitive decline trajectories.

3. Methods

3.1 Study Cohort and Sample Selection

The University of Manchester Longitudinal Study of Cognition in Normal Healthy Old Age recruited 6,542 volunteers (aged 42–92) between 1983–1994 through advertising in Greater Manchester and Newcastle, excluding those with overt cognitive impairment or dementia (Robinson et al., 2020). Of 6,356 participants completing four assessment waves at four-year intervals, 1,563 had genome-wide genotyping (Illumina Human 610-Quad BeadChip; Didikoglu et al., 2022). The final analytic sample comprised 434 participants with complete genotype, cognitive-trajectory, and covariate data after merging files and excluding missing values. Participant characteristics are in Tables 1 and 2.

3.2 Genetic Data: Selection, Quality Control, and Preparation

Candidate Gene Selection

Dopaminergic neurotransmission genes were grouped into four categories: receptors (DRD1, DRD2, DRD3, DRD4, DRD5), synthesis (TH, DDC), clearance (SLC6A3/DAT1, MAOA, MAOB), and metabolism/modulation (COMT, PPP1R1B, DBH).

SNP Identification and Quality Control

Common SNPs within candidate genes were identified using NCBI Variation Viewer (GRCh38.p14), filtering for variants from dbSNP with a minor allele frequency (MAF) of $\geq 1\%$ within gene boundaries. Subsequently, 1,363 SNPs across 13 prespecified genes were extracted from the genome-wide association study database.

Of the 13 prespecified genes, four were excluded: MAOA, MAOB, and DRD4 (no variants found on the genotyping array) and DRD5 (single variant failed MAF $< 5\%$ threshold). The remaining data underwent stringent quality control using PLINK v1.9, which applied the following criteria: exclusion of individuals with $> 2\%$ missing genotypes and SNPs with $> 2\%$ missing data, a MAF $< 5\%$ within the study cohort, or a Hardy-Weinberg equilibrium deviation ($p < 1 \times 10^{-4}$). The final analysis therefore included 957 SNPs from the following nine autosomal genes: COMT, DRD1, DRD2, DRD3, TH, DDC, SLC6A3, DBH, and PPP1R1B. Detailed QC results are presented in Appendix A1.

Dataset Integration and Population Structure

Following quality control, the nine gene datasets were merged into a single analysis file using PLINK. Cognitive phenotype data were then integrated, ensuring missing values were correctly handled. Finally, 20 ancestry principal components were computed from the 957-SNP genotype panel.

3.3 Cognitive Battery and Domain Assessment

Cognitive abilities were evaluated across four domains using 12 pencil-and-paper tests (three per domain) at four waves spanning 12 years. Processing speed: visual search, alphabet-coding (Savage, 1984), semantic-reasoning (Baddeley, Emslie, & Nimmo-Smith, 1992). Fluid reasoning: Heim AH4-1/AH4-2 (Heim, 1970), Culture Fair Intelligence Test (Cattell & Cattell, 1960). Verbal memory: free/cumulative/delayed recall of six-letter nouns. Visual memory: picture-recognition, memory-for-objects, shape-location recall. Full administration details in Rabbitt et al. (2004).

Choice of Primary and Secondary Cognitive domains

Processing speed was the primary domain due to its central role in cognitive aging and strong dopaminergic links. Other domains were secondary outcomes assessing effect specificity. Decline rates (slopes) were primary outcomes reflecting aging processes; performance at age 70 (intercepts) was secondary.

3.4 Cognitive Trajectory Modeling and Outcome Definition

Individual cognitive trajectories were modeled using multilevel growth curves (Aichele et al., 2016) over the 12-year study period, with age centered at 70 years. Best Linear Unbiased Predictors (BLUPs) for intercepts (performance at age 70) and slopes (annual change rates) served as outcomes in all subsequent genetic association analyses.

3.5 Covariates

Covariate selection was guided by established relationships with cognitive outcomes to control for potential confounding and improve precision of genetic associations.

3.5.1 Core Covariates

Sex: Coded as 0 = Female, 1 = Male

Ancestry principal components (PC1-PC20): Included to control for population stratification, which prevents spurious findings that can arise from subtle ancestral differences within the study cohort.

3.5.2 Clinical Covariates

Baseline values from the initial clinical visit were used for all covariates to ensure consistency.

Baseline Depression Score: Measured using the Beck Depression Inventory (Beck et al., 1961). Late-life depression is a significant risk factor for cognitive impairment and is associated with a faster rate of cognitive decline (Pellegrino et al., 2013).

Hypertension status (diagnosed OR clinic SBP \geq 140 mm Hg / DBP \geq 90 mm Hg): Defined by self-report or clinical readings, hypertension is a prevalent risk factor for cognitive decline in older adults, particularly impacting processing speed (Walker et al., 2017).

Mean Arterial Pressure (MAP): Calculated from the mean of three diastolic and systolic readings ($MAP = DBP + \frac{1}{3} \times [SBP - DBP]$). Included as a continuous measure of the aforementioned vascular risk.

Body Mass Index (BMI): Provided directly in the dataset as kg/m^2 , instability in BMI (both significant gain and loss) is a robust predictor of accelerated cognitive decline in older adults (Beeri et al., 2022).

3.5.3 Lifestyle and Sleep Covariates

Smoking Status: A binary variable for current smokers versus non-smokers, as smoking is a risk factor for cognitive decline (Anstey et al., 2007).

Alcohol Consumption Frequency: The estimated number of drinking occasions per week, excessive alcohol consumption is associated with a faster rate of cognitive decline in midlife and beyond (Sabia et al., 2014).

Physical Activity: Total weekly minutes of combined moderate and vigorous activity, which is known to protect against cognitive decline (Angevaren et al., 2008).

Sleep Duration: Average self-reported hours of sleep per night, as both short (≤ 5 hours) and long (≥ 9 hours) sleep durations are linked to cognitive deficits (Lo et al., 2016)

Sleep Efficiency: Self-reported as a percentage. Low sleep efficiency is an indicator of poor sleep, which is a known risk factor for cognitive dysfunction (Jiang et al., 2024).

Self-Rated Health: An ordinal variable on a 5-point scale from "Poor" (1) to "Excellent" (5), poor self-rated health is a predictor of adverse health outcomes and is directly associated with accelerated cognitive decline (Ramsingh et al., 2024).

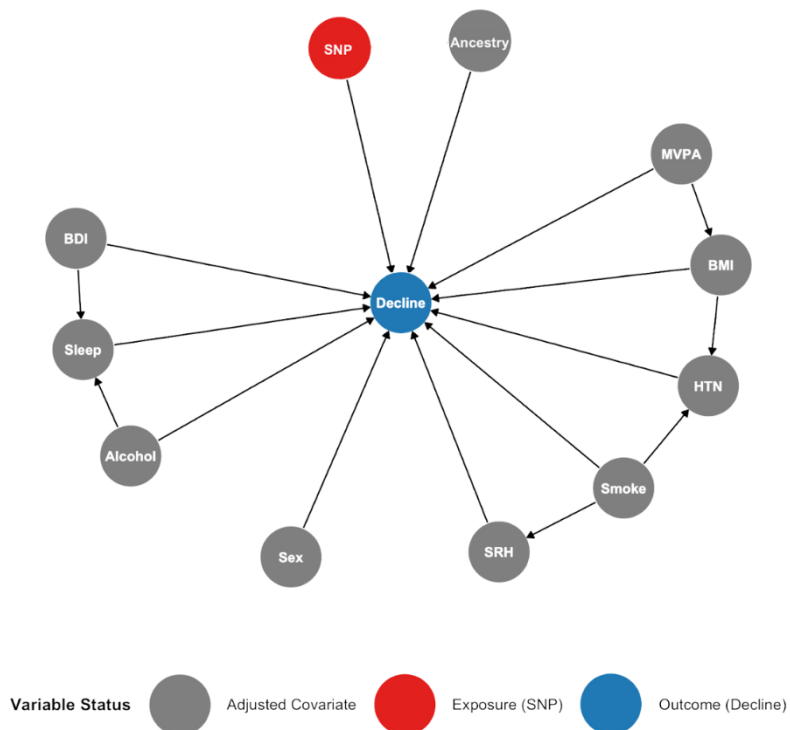
3.5.4 Additional Ancestry Principal Components

To evaluate the stability of results under different levels of population stratification control, association models were tested using PC1-3, PC1-10, and PC1-20 specifications, with optimal adjustment determined through model diagnostics (detailed in Section 3.7.1).

3.5.5 DAG-Based Covariate Selection

To isolate the direct genetic effect on cognitive decline, a Directed Acyclic Graph (DAG) was developed (Figure 4). This simplified model formalizes causal assumptions from the literature to identify a sufficient set of confounders (ancestry, clinical indicators, and lifestyle factors) for adjustment, thereby blocking non-causal "backdoor" pathways while avoiding over-adjustment bias.

Figure 4. Directed Acyclic Graph for the Effect of Dopamine Gene Variants on Processing Speed Decline.



Assumed causal pathways between genetic variants (Exposure-SNP) and processing speed decline (Outcome). Grey nodes represent covariates blocking confounding pathways; arrows indicate hypothesized causal effects.

3.6 Missing Data Handling

Of the 6,542 participants in the full longitudinal cohort, 1,563 had genome-wide genotyping data. A structural pattern of missing data was identified, with approximately half the participants, predominantly from the Newcastle site, lacking

clinical data (blood pressure, BMI, lifestyle factors) collected only during optional on-site visits.

The main analysis prioritized internal validity over sample size. Although 1,179 genotyped individuals had cognitive trajectory data, the analytic sample was restricted to 434 participants with complete clinical assessments to avoid systematic bias from omitting crucial confounders, a trade-off formally tested in sensitivity analysis.

Data missingness patterns were visualized, and Little's MCAR test supported a Missing At Random (MAR) assumption for variables with <50% missingness. Covariates with <5% missing data used complete-case analysis, while those with ≥5% missingness were imputed. Two variables, BDI mood score (5.7% missing) and alcohol frequency (17.2% missing), underwent multiple imputation using the mice package in R (20 iterations, predictive mean matching), with the imputation model including all analysis covariates to maintain multivariate relationships.

Model Diagnostics and Assumption Testing

Prior to genetic association analysis, comprehensive model diagnostics ensured statistical validity. Covariate-only models were evaluated for multicollinearity (variance inflation factors < 5.0), normality of residuals (Q-Q plots), and homoscedasticity (residuals versus fitted values plots with LOESS curves), generated using the qqman package (Turner, 2018). After replacing individual blood pressure measures with mean arterial pressure (MAP) to resolve severe multicollinearity (VIFs > 35), no covariate exceeded the conservative threshold of 5, confirming acceptable independence among predictors. Model convergence was verified for all regression specifications.

Regression assumptions were evaluated using covariate-only models across three principal component specifications (PC1-3, PC1-10, PC1-20), confirming assumptions were met prior to genetic association testing.

3.7 Genetic Association Analyses

3.7.1 Single SNP Association Analysis

Candidate-gene analyses were conducted on 957 SNPs from nine dopamine pathway genes (TH, DDC, DRD1, DRD2, DRD3, SLC6A3, COMT, DBH, PPP1R1B), using a sample of 1,563 participants with genotype data and 434 with cognitive trajectory data.

All analyses were performed using linear regression in PLINK v1.9 (Chang et al., 2015; <https://zzz.bwh.harvard.edu/plink>) under an additive genetic model, consistently adjusting for sex, ancestry principal components (PC1–PC20), and clinical covariates.

The analyses were structured into three tiers:

Primary Analysis: Processing speed slope (gsstd_lin), representing annual change in standard deviation units from age 70.

$$\text{gsstd_lin} = \beta_0 + \beta_1 \cdot \text{SNP} + \beta_2 \cdot \text{Sex} + \beta_3 \cdot \text{Hypertension_Status} + \beta_4 \cdot \text{Smoking} + \beta_5 \cdot \text{BMI} + \beta_6 \cdot \text{MAP} + \beta_7 \cdot \text{BDI_Score} + \beta_8 \cdot \text{Alcohol_Frequency} + \beta_9 \cdot \text{MVPA} + \beta_{10} \cdot \text{Sleep_Hours} + \beta_{11} \cdot \text{Sleep_Efficiency} + \beta_{12} \cdot \text{Self_Rated_Health} + \beta_{13} \cdot \text{PC1} + \beta_{14} \cdot \text{PC2} + \dots + \beta_{32} \cdot \text{PC20} + \varepsilon$$

(*gsstd_lin* is the outcome variable, β_0 is the intercept, β_i represents regression coefficients, SNP is the genetic variant coded additively (0, 1, 2), and ε is the error term.)

Secondary Slope Analyses: Fluid reasoning (gfstd_lin), episodic memory (gmstd_lin), and vocabulary (gvstd_lin) slopes to evaluate domain-specificity of dopaminergic genetic effects on cognitive decline.

Secondary Intercept Analyses: Processing speed (gsstd_int), fluid reasoning (gfstd_int), episodic memory (gmstd_int), and vocabulary (gvstd_int) intercepts to investigate dopaminergic genetic effects on cognitive performance at age 70.

All association analyses were adjusted for sex, ancestry principal components, and clinical covariates.

Population Stratification Control and Model Selection

Population stratification control was optimized by comparing genomic control inflation factors (λ_{GC}) across three PC specifications (PC1–3, PC1–10, PC1–20). PC1–20 was selected based on adequate calibration ($\lambda_{\text{GC}} \approx 1.033$), assessed via genomic control factors and quantile-quantile plots. All subsequent analyses employed PC1–20 for population structure adjustment.

Multiple testing correction

A hierarchical multiple testing correction strategy was applied for SNP-level tests. For the 957 SNP-level tests across all cognitive domains, both Bonferroni ($\alpha \approx 5.22 \times 10^{-5}$) and Benjamini-Hochberg FDR ($q < 0.05$) corrections were used consistently for both slope and intercept analyses.

Power Considerations

Given the restricted sample size (N=434), statistical power limitations motivated a sensitivity analysis to evaluate robustness of findings in a larger sample.

Clinical Data Restriction Sensitivity Analysis

To assess whether restricting the sample to participants with complete clinical data influenced genetic association results, a sensitivity analysis was conducted on the full genotyped sample (N=1,179) for processing speed slope associations.

The main analysis included only Manchester participants with clinical assessments, while this sensitivity analysis included both Manchester and Newcastle sites. Study site was added as a covariate to control for site-specific differences. Due to systematic absence in Newcastle participants, clinical covariates were excluded: Beck Depression Inventory score, MAP, hypertension status, and body mass index.

Statistical methods were identical to the primary analysis; only the covariate set was modified for available data across the larger sample.

The linear regression model was:

$$\text{gsstd_lin} = \beta_0 + \beta_1 \cdot \text{SNP} + \beta_2 \cdot \text{Sex} + \beta_3 \cdot \text{Site} + \beta_4 \cdot \text{Smoking} + \beta_5 \cdot \text{Alcohol_Frequency} + \beta_6 \cdot \text{MVPA} + \beta_7 \cdot \text{Sleep_Hours} + \beta_8 \cdot \text{Sleep_Efficiency} + \beta_9 \cdot \text{Self_Rated_Health} + \beta_{10} \cdot \text{PC1} + \beta_{11} \cdot \text{PC2} + \dots + \beta_{29} \cdot \text{PC20} + \varepsilon$$

(Site represents participant recruitment location.)

This sensitivity model enabled direct comparison of the trade-off between sample size maximization and clinical confounder control.

3.7.2 Gene-Based and Pathway-Level Analyses

Gene-Based Testing: Cumulative variant effects for eight dopamine pathway genes were assessed using MAGMA v1.10 (de Leeuw et al., 2015; <https://cnrc.nl/research/magma/>). The analysis aggregated single-SNP statistics on all cognitive slopes and intercepts via a SNP-wise mean model, with linkage disequilibrium estimated from the 1000 Genomes European panel. TH was excluded due to insufficient SNP coverage. Statistical significance was set at a Bonferroni-corrected threshold of $\alpha = 0.00625$.

Dopamine Polygenic Risk Score: To measure aggregate pathway effects, a dopamine polygenic risk score (dPRS) was constructed. The initial 957 variants from nine genes were pruned for linkage disequilibrium ($r^2 > 0.10$; PLINK v1.9), leaving 25 quasi-independent variants. The dPRS was based on unweighted allele counting and was z-standardized before being tested against cognitive slopes and intercepts across all domains.

3.7.3 Exploratory Pathway Component Analysis: Genetic Associations with Neuropathology and Synaptic Density

Sample Characteristics and Data Availability

Post-mortem brain tissue data were available for 148 participants for neuropathological analysis. A subset of 61 participants had synaptic density measurements across multiple brain regions.

Neuropathological Markers

Primary Neuropathological Markers: Three markers were analyzed as continuous variables: Braak Stage (tau pathology), Thal Phase (amyloid- β plaques), and Cerebral Amyloid Angiopathy (CAA). CERAD Score was excluded due to $>75\%$ missingness.

Exploratory Neuropathological Markers: Two binary markers were examined: α -Synuclein Pathology and TDP-43 Inclusions. All assessments followed established diagnostic criteria.

Synaptic Density Measurements

Synaptic density was measured across five brain regions, with the frontal cortex serving as the primary measure. Additional regions included the hippocampus, temporal, parietal, and occipital cortex. All measures were continuous.

Missing Data and Sample Preparation

Distinct missing data handling protocols were established for the neuropathology and synaptic density post-mortem datasets due to differences in sample size and data availability.

Neuropathology Data: From an initial 148 participants, variables with $>75\%$ missingness (CERAD) were excluded. Multiple imputation by chained equations (MICE) was performed using 20 iterations with predictive mean matching for variables

with 5-75% missingness, including CAA score (14.2% missing), alcohol frequency (12.2% missing), and post-mortem interval (5.4% missing). Variables with <5% missingness underwent complete case analysis, resulting in a final sample of n=116 for the basic model.

Synaptic Density Data: From an initial 61 participants, 8 were excluded for lacking genetic data. Complete case filtering was applied to variables with <5% missingness. MICE was performed using 20 iterations with predictive mean matching for remaining variables with 5-75% missingness (frontal cortex, hippocampus, and parietal cortex density; alcohol frequency; post-mortem interval), yielding a final analysis sample of n=50.

Covariate Selection and Justification

Systematic Covariate Testing: Two covariate approaches were tested: a full model (n=60, 30+ covariates) and a basic model (n=116, streamlined covariates).

Testing Results: The full model failed to converge due to the small sample size relative to the number of parameters. The basic model successfully converged for continuous outcomes.

Final Covariate Strategy: Power analyses established detectable effect size thresholds for post-mortem datasets. The basic covariates approach (n=116) used PC1-20 ancestry adjustment from the main analysis. Continuous outcomes (Braak, Thal, CAA) employed the full basic covariate set, while binary outcomes (α -synuclein, TDP-43) used minimal covariates due to rare events. For synaptic density analysis (n=50), multicollinearity was resolved by creating a composite Sleep_Quality score, reducing maximum VIF to 4.07.

Consistent Application: This empirically-determined basic covariates strategy was applied consistently across all pathway component analyses.

Model Diagnostics and Assumption Testing

Prior to analysis, covariate-only models were checked for multicollinearity (VIFs < 5.0) and normality (Q-Q plots). Model convergence was assessed for all linear and logistic regression models.

Statistical Models and Analytical Framework

Exploratory analyses investigated neurobiological mechanisms of the hypothesized dopaminergic pathway using post-mortem brain tissue data, deconstructing the

proposed dopamine genes → brain pathology → cognitive decline pathway into two testable components:

Component 1: Genetic-Neuropathology and Synaptic Density Association Models

This component tested direct associations between 957 dopaminergic variants and post-mortem neuropathological and synaptic markers to determine if genetic variation influences brain biology independently of cognitive outcomes.

Continuous Neuropathological Markers (Braak, Thal, CAA):

$$\text{Outcome} = \beta_0 + \beta_1 \cdot \text{SNP} + \beta_2 \cdot \text{Sex} + \beta_3 \cdot \text{Site} + \beta_4 \cdot \text{PC1} + \beta_5 \cdot \text{PC2} + \dots + \beta_{23} \cdot \text{PC20} + \beta_{24} \cdot \text{Age_at_Death} + \beta_{25} \cdot \text{PMI} + \beta_{26} \cdot \text{APOE_e4} + \beta_{27} \cdot \text{Smoke_Current} + \beta_{28} \cdot \text{Alcohol_Frequency} + \beta_{29} \cdot \text{MVPA} + \beta_{30} \cdot \text{Sleep_Hours} + \beta_{31} \cdot \text{Sleep_Efficiency} + \beta_{32} \cdot \text{Self_Rated_Health} + \varepsilon$$

(*PMI* is post-mortem interval; *APOE_e4* indicates ≥1 APOE e4 alleles.)

Binary Neuropathological Markers (α -Synuclein, TDP-43):

$$\text{logit}[P(\text{pathology} = 1)] = \beta_0 + \beta_1 \cdot \text{SNP} + \beta_2 \cdot \text{Sex} + \beta_3 \cdot \text{Age_at_Death} + \beta_4 \cdot \text{PMI} + \beta_5 \cdot \text{APOE_e4} + \beta_6 \cdot \text{PC1} + \beta_7 \cdot \text{PC2} + \beta_8 \cdot \text{PC3}$$

(*logit[P(pathology = 1)]* is the log-odds of the presence of the binary neuropathological marker.)

Continuous Outcomes (Synaptic Density):

$$\text{Synaptic_Density} = \beta_0 + \beta_1 \cdot \text{SNP} + \beta_2 \cdot \text{Sex} + \beta_3 \cdot \text{Site} + \beta_4 \cdot \text{PC1-PC20} + \beta_{24} \cdot \text{Age_at_Death} + \beta_{25} \cdot \text{PMI} + \beta_{26} \cdot \text{APOE_e4} + \beta_{27} \cdot \text{Smoke_Current} + \beta_{28} \cdot \text{Alcohol_Frequency} + \beta_{29} \cdot \text{MVPA} + \beta_{30} \cdot \text{Sleep_Quality} + \beta_{31} \cdot \text{Self_Rated_Health} + \varepsilon$$

(*Sleep_Quality* is a composite score from sleep duration and efficiency.)

Component 2: Neuropathology-Cognition Association Models

This component examined whether brain pathology markers predicted cognitive decline rates, validating cognitive measures' sensitivity to underlying neuropathology. Secondary analysis assessed links between brain markers and cognitive intercepts at age 70.

$$(\text{gsstd_lin/gsstd_int}) = \beta_0 + \beta_1 \cdot \text{Brain_Pathology_Marker} + \beta_2 \cdot \text{Sex} + \beta_3 \cdot \text{Site} + \beta_4 \cdot \text{Age_at_Death} + \beta_5 \cdot \text{PMI} + \beta_6 \cdot \text{APOE_e4} + \beta_7 \cdot \text{Smoke_Current} + \beta_8 \cdot \text{Alcohol_Frequency} + \beta_9 \cdot \text{MVPA} + \beta_{10} \cdot \text{Sleep_Hours} + \beta_{11} \cdot \text{Sleep_Efficiency} + \beta_{12} \cdot \text{Self_Rated_Health} + \varepsilon$$

Multiple Testing Correction

A hierarchical multiple testing strategy was used to control for Type I error.

For Component 1: The 957 SNP tests for each post-mortem outcome were corrected using a Bonferroni threshold ($\alpha \approx 5.22 \times 10^{-5}$) and a Benjamini-Hochberg False Discovery Rate (FDR) of $q < 0.05$.

For Component 2: An FDR of $q < 0.05$ was applied within distinct families of tests (e.g., primary markers vs. cognitive slopes, primary markers vs. intercepts).

Power Considerations

Power analyses were conducted for the post-mortem datasets to establish detectable effect size thresholds.

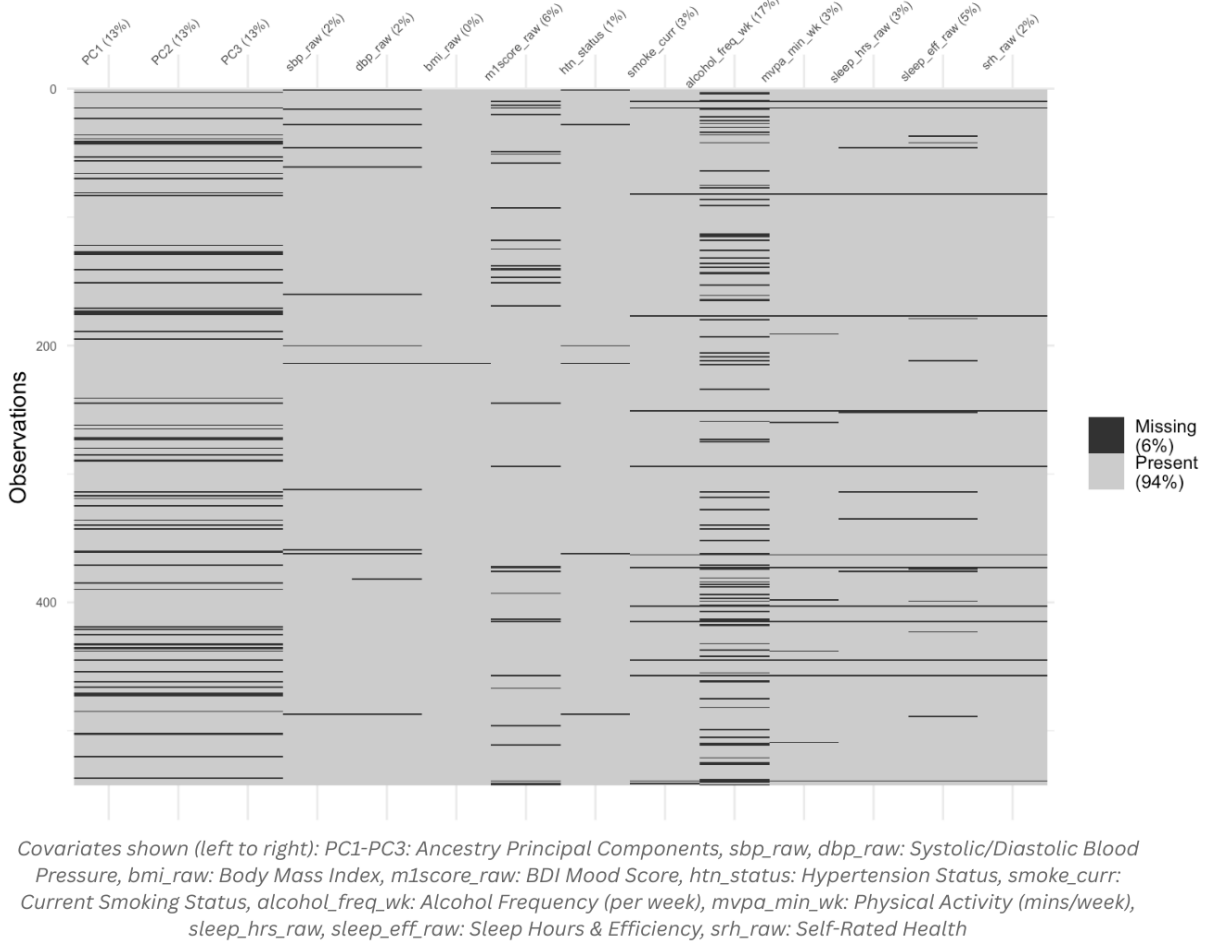
4. Results

4.1 Exploratory Data Analysis

4.1.1 Missing Data Overview

The analysis was based on 542 participants with key clinical covariate data, for whom missing data patterns are illustrated in Figure 5. Little's MCAR test indicated data were missing completely at random ($\chi^2 = 280.0$, $df = 296$, $p = 0.74$). Most covariates with less than 5% missingness were handled via complete-case analysis. Two variables with higher missingness, baseline BDI mood score (5.7%) and alcohol frequency (17.2%), were imputed using multiple imputation. Imputation diagnostics confirmed the validity of this approach (Appendix A2). This combined process resulted in a final analytic sample of 434 participants with complete covariate data for all subsequent analyses.

Figure 5. Missing-Data Heat-Map for Covariates (N=542).



Heat-map illustrating the pattern of missing data across all covariates in the initial sample. Light gray indicates observed data; black indicates missing.

4.1.2 Participant Characteristics

The final analytic cohort (N=434) was predominantly female (69%) and characterized by a high prevalence of hypertension (87%), but otherwise presented with generally healthy baseline lifestyle and clinical indicators, as detailed in Table 1.

Table 1. Participant Characteristics of the Analytic Sample (N = 434).

Participant Characteristics

Categorical (n %)	
Sex	Female n=301 (69%), Male n=133 (31%)
Hypertension status	Normotensive n=57 (13%), Hypertensive n=377 (87%)
Smoking status	Non-smoker n=383 (88%), Current smoker n=51 (12%)
Continuous (median [IQR])	
BMI (kg/m ²)	25.39 [23.11, 28.04]
Systolic BP (mm Hg)	110.64 [102.46, 119.25]
Diastolic BP (mm Hg)	99.93 [92.89, 107.68]
BDI mood score	5.00 [2.00, 9.00]
Alcohol freq. (wk ⁻¹)	0.67 [0.46, 0.77]
MVPA (min wk ⁻¹)	275.99 [110.40, 496.78]
Sleep hours (h)	7.00 [6.50, 8.00]
Sleep efficiency (%)	86.58 [79.56, 92.31]
Self-rated health	4.00 [4.00, 5.00]

Abbreviations: BP, blood pressure; BDI, Beck Depression Inventory; MVPA, moderate-to-vigorous physical activity; IQR, interquartile range.

Data are n (%) for categorical variables or median [interquartile range] for continuous variables. All measures are from baseline.

4.1.3 Cognitive Trajectory Outcomes

The primary outcomes were 12-year cognitive trajectories, defined by slopes (annual change) and intercepts (performance at age 70). As detailed in Table 2, decline rates were steepest for processing speed (median = 0.48 SD/year). While intercepts showed comparable variation across domains, the decline slope for processing speed exhibited the greatest individual differences (IQR = 1.70 SD units), supporting its selection as the primary outcome.

Table 2. Median cognitive-trajectory slopes and intercepts by domain in the Analytic Sample (N=434).

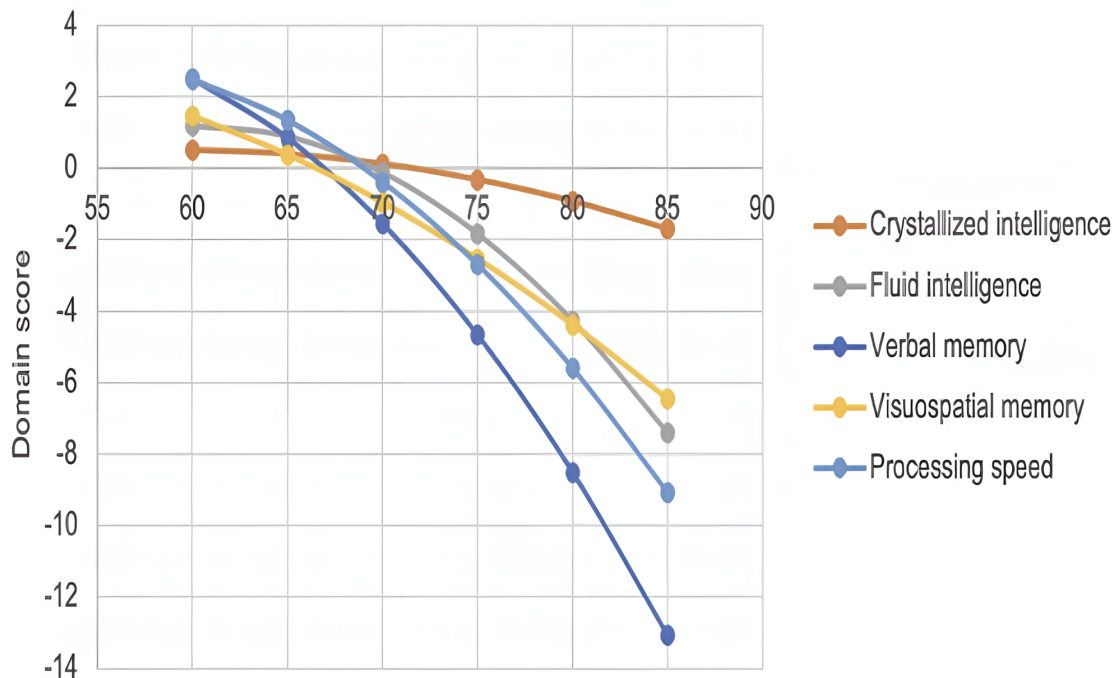
Cognitive Outcomes	
Cognitive-slope outcomes (median [IQR])	
Processing-speed slope	0.48 [-0.35, 1.35]
Fluid-reasoning slope	0.46 [-0.34, 1.15]
Vocabulary slope	0.15 [-0.58, 0.70]
Episodic-memory slope	0.14 [-0.68, 0.81]
Cognitive-intercept outcomes (median [IQR])	
Processing-speed intercept	0.55 [-0.09, 1.19]
Fluid-reasoning intercept	0.63 [-0.06, 1.28]
Vocabulary intercept	0.43 [-0.23, 1.02]
Episodic-memory intercept	0.52 [-0.22, 1.20]

Abbreviations: IQR, interquartile range.

Summary of cognitive-trajectory parameters (in SD units) derived from linear mixed-effects models. Slopes represent annual change; intercepts represent performance at age 70.

The individual-level trajectories reported here are consistent with established population-level aging patterns from the same cohort, as illustrated in Figure 6 (Ourania Sfakianaki, In press, 2025). This visualization highlights the steep decline of processing speed relative to the marked stability of crystallized intelligence, reinforcing the selection of processing speed as the primary study outcome.

Figure 6. Mean trajectories of cognitive domains from age 60 to 85 (provided by Ourania Sfakianaki, In press, 2025).



Domain scores in standard deviation (SD) units plotted by age. Each line represents the mean trajectory for one of five cognitive domains.

4.2 Single SNP Associations with Cognitive Decline and Performance

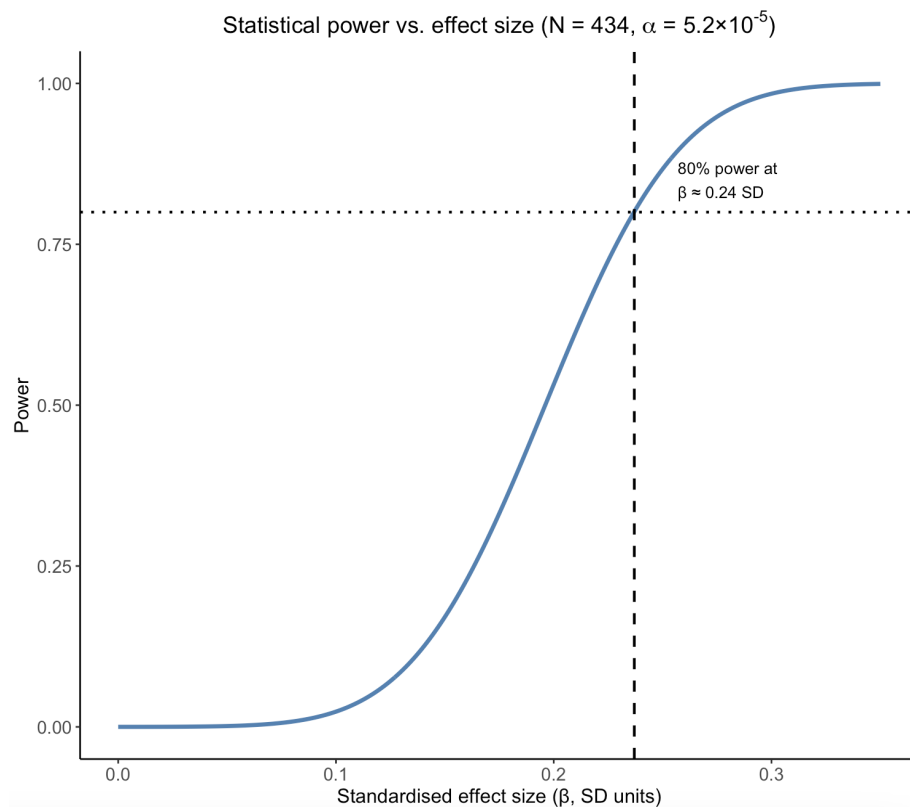
4.2.1 Covariate Diagnostics and Population-Structure Adjustment

Preliminary model diagnostics confirmed all regression assumptions were met. Multicollinearity was resolved using mean arterial pressure (VIF < 2.2), and diagnostic plots showed residuals that were normally distributed without evidence of heteroscedasticity, despite the presence of three outliers (Appendix A3). For population structure, a 20-principal-component (PC1–20) adjustment was selected, as its genomic inflation factor ($\lambda_{GC} = 1.03$) demonstrated superior calibration over inflated models using fewer PCs (PC1–3 and PC1–10; $\lambda_{GC} = 1.37$ – 1.81). The corresponding quantile-quantile (QQ) plot confirmed this robust calibration (Appendix A4), validating the use of the PC1–20 model for all subsequent analyses.

4.2.2 Statistical power to detect single-variant effects

The primary analysis ($N=434$) had 80% power to detect single-variant effects of $\beta \geq 0.24$ standard deviations (SD) per allele, corresponding to a variant explaining $\approx 5.3\%$ of the variance in the processing-speed slope, at a Bonferroni-corrected significance threshold of $\alpha = 5.2 \times 10^{-5}$ (Figure 7).

Figure 7. Power curve for single-SNP association tests ($N=434$, $\alpha = 5.2 \times 10^{-5}$, two-sided).



Statistical power as a function of standardized per-allele effect size (β , in SD units). The horizontal line indicates 80% power; the vertical line indicates the corresponding effect size.

4.2.3 Sensitivity Analysis: Full Sample with Modified Covariates

The use of the smaller, well-calibrated primary analysis was validated by a sensitivity test on the larger, less-adjusted sample ($N=1,179$). While also null with the same top signal location (Chr22 cluster), this larger analysis produced significant genomic

deflation ($\lambda_{GC} = 0.813$; Table 3), reflecting an ~19% downward bias that negated the benefit of using the larger sample size..

Table 3. Comparison of Primary and Sensitivity Analyses for Processing Speed Slopes.

Analysis	Sample Size	Covariate Set	Top Signal Location	Minimum P-value	Bonferroni Significant	Lambda GC
Primary Analysis	n = 434	Clinical + Demographics + PC1-20	Chr22 cluster	8.4×10^{-3}	0	1.03
Sensitivity Analysis	n = 1,179	Demographics + Lifestyle + Site + PC1-20	Chr22 cluster	3.88×10^{-3}	0	0.813

Abbreviations: Chr, chromosome; GC, genomic control.

Methodological summary illustrating the trade-off between the primary model's comprehensive covariate adjustment and the sensitivity analysis's larger sample size.

4.2.4 SNP Associations with Processing Speed Decline

Single-SNP analyses of 957 dopaminergic variants revealed no significant associations with the rate of processing speed decline after a pathway-wide Bonferroni and FDR correction.

The top 10 nominal signals are detailed in Table 4 to illustrate the data's characteristics. Notably, many of these signals clustered within the COMT gene, while the leading variant, rs3025383, is located in the DBH gene. This top variant was characterized by a large but statistically imprecise effect estimate ($\beta = -0.79$ SD; 95% CI [-1.38, -0.21]; $p = 0.008$). However, all variants remained non-significant after FDR correction (smallest $q = 0.844$). The overall distribution of these null findings across the dopamine pathway is visualized in Figure 8.

Table 4. Top 10 variants for processing speed slopes ranked by raw p-value (PC1-20 model).

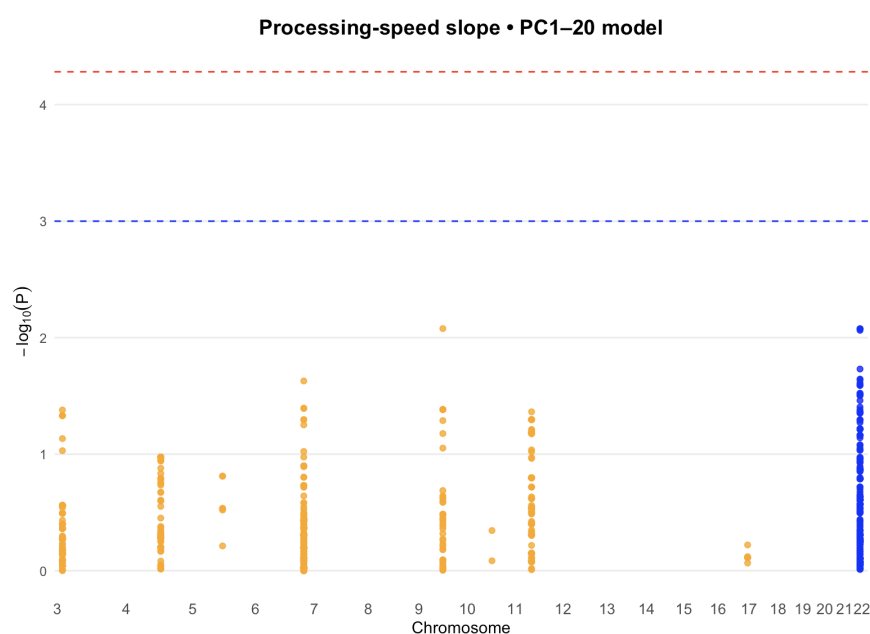
PRIMARY: Processing Speed SLOPES (Decline Rate)

Chr	SNP ID	Gene	Effect		A2	EAF	β (SD)	SE	L95	U95	Raw P-value	P_bonf	q (FDR)
			Allele										
9	rs3025383	DBH	C	T	0.186	0.7944	0.2995	-1.3814	-0.2074	0.008		1	0.844
22	rs2238791	COMT	A	C	0.472	1.0180	0.3842	0.2650	1.7710	0.008		1	0.844
22	rs2531693	COMT	G	C	0.472	1.0180	0.3842	0.2650	1.7710	0.008		1	0.844
22	rs2106140	COMT	A	G	0.472	1.0180	0.3842	0.2650	1.7710	0.008		1	0.844
22	rs2238790	COMT	G	A	0.321	-0.7268	0.2754	-1.2666	-0.1870	0.009		1	0.844
22	rs165815	COMT	C	T	0.125	-0.5527	0.2338	-1.0109	-0.0945	0.019		1	0.844
22	rs2073746	COMT	T	C	0.213	-0.7345	0.3210	-1.3637	-0.1053	0.023		1	0.844
22	rs2073747	COMT	A	G	0.214	-0.7137	0.3126	-1.3264	-0.1010	0.023		1	0.844
7	rs6593011	DDC	A	C	0.142	0.6282	0.2763	0.0867	1.1697	0.024		1	0.844
22	rs887199	COMT	A	G	0.123	-0.5341	0.2364	-0.9974	-0.0708	0.024		1	0.844

Abbreviations: Chr, chromosome; A2, other allele; EAF, effect allele frequency; β (SD), effect size in standard deviation units; SE, standard error; L95/U95, 95% confidence interval; P_bonf, Bonferroni-corrected p-value; q(FDR), false discovery rate.

Top 10 genetic associations with processing speed decline rate, ranked by uncorrected p-value.
Results are from the primary, fully-adjusted model (PC1–20).

Figure 8. Manhattan plot for processing speed slopes (PC1–20 model).



Association p-values for 957 SNPs with the processing speed slope. The red dashed line indicates the Bonferroni significance threshold ($P = 5.22 \times 10^{-5}$), while the blue dashed line indicates the threshold for suggestive significance ($P = 1 \times 10^{-3}$).

4.2.5 Associations with Secondary Cognitive Domains (Slopes)

The null finding extended beyond processing speed, as no significant associations were found for any secondary cognitive decline slope after pathway-wide Bonferroni and FDR correction. To illustrate this robust null pattern, the strongest nominal signal was for a DRD1 variant (rs12518222, $p = 0.002$) associated with fluid reasoning decline, which remained highly non-significant (FDR $q = 0.84$). This pervasive lack of association suggests the null result is a general characteristic of this genetic pathway and not an artifact of phenotype selection. Full results for all secondary domains are provided in Appendix A5.

4.2.6 SNP Associations with Cognitive Intercepts

Associations with baseline cognitive performance were assessed using intercepts at age 70. Consistent with the decline rate analysis, no variant was significantly associated with processing speed intercepts after multiple testing correction (all FDR $q > 0.86$). The top nominal signals, detailed in Table 5, clustered within the COMT gene and were rendered non-significant by low precision. For example, the leading COMT variant (rs165656) had a wide confidence interval that only narrowly excluded zero ($\beta = -0.30$ SD; 95% CI [-0.53, -0.08]; $p = 0.009$). This overall null result is visualized in the Manhattan plot in Figure 9.

Table 5. Top 10 variants for processing speed intercepts ranked by raw p-value.

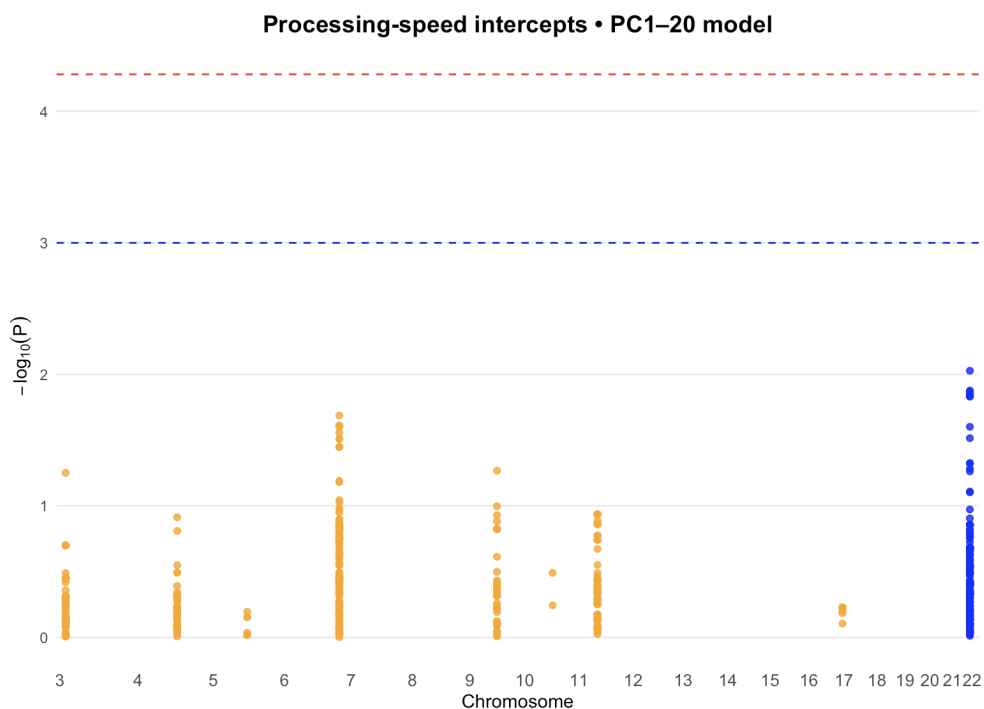
PRIMARY: Processing Speed INTERCEPTS (Performance at Age 70)

Chr	SNP ID	Gene	Effect		A2	EAF	β (SD)	SE	L95	U95	Raw P-value	P_bonf	q(FDR)
			Allele	A2									
22	rs165656	COMT	G	C	C	0.478	-0.3037	0.1163	-0.5316	-0.0758	0.009	1	0.861
22	rs4818	COMT	G	C	C	0.414	-0.2919	0.1173	-0.5218	-0.0620	0.013	1	0.861
22	rs740601	COMT	G	T	0.415	-0.2895	0.1167	-0.5182	-0.0608	0.014	1	0.861	
22	rs165722	COMT	C	T	0.480	-0.2829	0.1149	-0.5081	-0.0577	0.014	1	0.861	
22	rs4633	COMT	C	T	0.480	-0.2829	0.1149	-0.5081	-0.0577	0.014	1	0.861	
22	rs4680	COMT	G	A	0.480	-0.2829	0.1149	-0.5081	-0.0577	0.014	1	0.861	
22	rs3810595	COMT	C	G	0.416	-0.2832	0.1156	-0.5098	-0.0566	0.015	1	0.861	
22	rs6269	COMT	G	A	0.416	-0.2832	0.1156	-0.5098	-0.0566	0.015	1	0.861	
22	rs2239393	COMT	G	A	0.416	-0.2832	0.1156	-0.5098	-0.0566	0.015	1	0.861	
7	rs2329371	DDC	A	G	0.212	0.7890	0.3394	0.1238	1.4542	0.021	1	0.861	

Abbreviations: Chr, chromosome; A2, other allele; EAF, effect allele frequency; β (SD), effect size in standard deviation units; SE, standard error; L95/U95, 95% confidence interval; P_bonf, Bonferroni-corrected p-value; q(FDR), false discovery rate.

Top 10 genetic associations with processing speed intercepts, ranked by uncorrected p-value. Results are from the primary, fully-adjusted model (PC1–20).

Figure 9. Manhattan plot for processing speed intercepts (PC1–20 model).



Association p-values for 957 SNPs with processing speed intercepts. The red dashed line indicates the Bonferroni significance threshold ($P = 5.22 \times 10^{-5}$), while the blue dashed line indicates the threshold for suggestive significance ($P = 1 \times 10^{-3}$).

4.2.7 SNP Associations with Secondary Cognitive Domains (Intercepts)

Analyses of secondary cognitive intercepts also yielded no significant associations after correction (all FDR $q > 0.74$). The pattern of large but statistically unstable nominal signals persisted, with the strongest being a DDC variant (rs11575429) associated with episodic memory. The consistent null finding across all cognitive outcomes, including both slopes and intercepts, suggests this is a general characteristic of the tested genetic pathway. Full results for each secondary cognitive domain are detailed in Appendix A6.

4.3 Gene-Based Association Testing

4.3.1 Gene-Based Associations with Processing Speed Decline

To test for cumulative genetic effects, a MAGMA gene-based analysis was performed. Reinforcing the single-variant results, no gene was significantly associated with processing speed decline after Bonferroni correction ($\alpha = 0.00625$). As detailed in Table 6, the top nominal signal was from the DRD2 gene ($Z = 0.765$, $p = 0.222$), which remained non-significant. This consistent null finding across both analyses suggests that these dopamine genes do not exert an effect large enough to be detected within this study's statistical power.

Table 6. Gene-based association results for processing speed slopes.

Processing Speed Slopes (PRIMARY)

Dopamine genes (N=434)					
Gene	N SNPs	Z-stat	P-value	P_bonf	q (FDR)
DRD2	117	0.765	0.222	1	0.786
DRD1	5	0.512	0.304	1	0.786
DBH	49	0.512	0.304	1	0.786
SLC6A3	104	0.157	0.438	1	0.786
COMT	43	-0.187	0.574	1	0.786
DRD3	105	-0.227	0.590	1	0.786
DDC	323	-0.620	0.732	1	0.837
PPP1R1B	8	-1.020	0.846	1	0.846

Abbreviations: N SNPs, number of variants in gene; Z-stat, MAGMA test statistic; P_bonf, Bonferroni-corrected p-value; q(FDR), false discovery rate.

Summary of gene-level association statistics for eight dopamine genes with processing speed decline. Genes are ranked by uncorrected p-value.

4.3.2 Gene-Based Associations with Secondary Cognitive Domains (Slopes)

No genes were significantly associated with decline in secondary cognitive domains after multiple testing correction. Although nominally significant associations emerged for DRD1 with fluid intelligence decline ($Z = 1.830$, $p = 0.034$) and PPP1R1B with fluid reasoning ($p = 0.050$) and vocabulary decline ($p = 0.050$), none approached statistical significance after correction (all FDR $q \geq 0.198$). The full findings, detailed in Appendix A7, suggest the null results are not specific to processing speed.

4.3.3 Gene-Based Associations with Processing Speed Intercepts

Gene-based testing of cognitive performance at age 70 (intercepts) also yielded null results. For processing speed, no gene achieved statistical significance after Bonferroni correction ($\alpha = 0.00625$). As shown in Table 7, COMT showed the strongest nominal association ($Z = 1.438$, $p = 0.075$), followed by DRD2 ($p = 0.304$), but all Bonferroni-adjusted p-values were non-significant.

Table 7. Gene-based association results for processing speed intercepts (performance at age 70).

Processing Speed Intercepts (PRIMARY)					
Dopamine genes (N=434)					
Gene	N SNPs	Z-stat	P-value	P_bonf	q (FDR)
COMT	43	1.438	0.075	0.601	0.601
DRD2	117	0.513	0.304	1.000	0.932
DDC	323	0.347	0.364	1.000	0.932
DBH	49	-0.192	0.576	1.000	0.932
PPP1R1B	8	-0.454	0.675	1.000	0.932
DRD3	105	-0.583	0.720	1.000	0.932
SLC6A3	104	-1.436	0.925	1.000	0.932
DRD1	5	-1.491	0.932	1.000	0.932

Abbreviations: N SNPs, number of variants in gene; Z-stat, MAGMA test statistic; P_bonf, Bonferroni-corrected p-value; q(FDR), false discovery rate.

Summary of gene-level association statistics for eight dopamine genes with processing speed intercepts. Genes are ranked by uncorrected p-value.

4.3.4 Gene-Based Associations with Secondary Cognitive Domains (Intercepts)

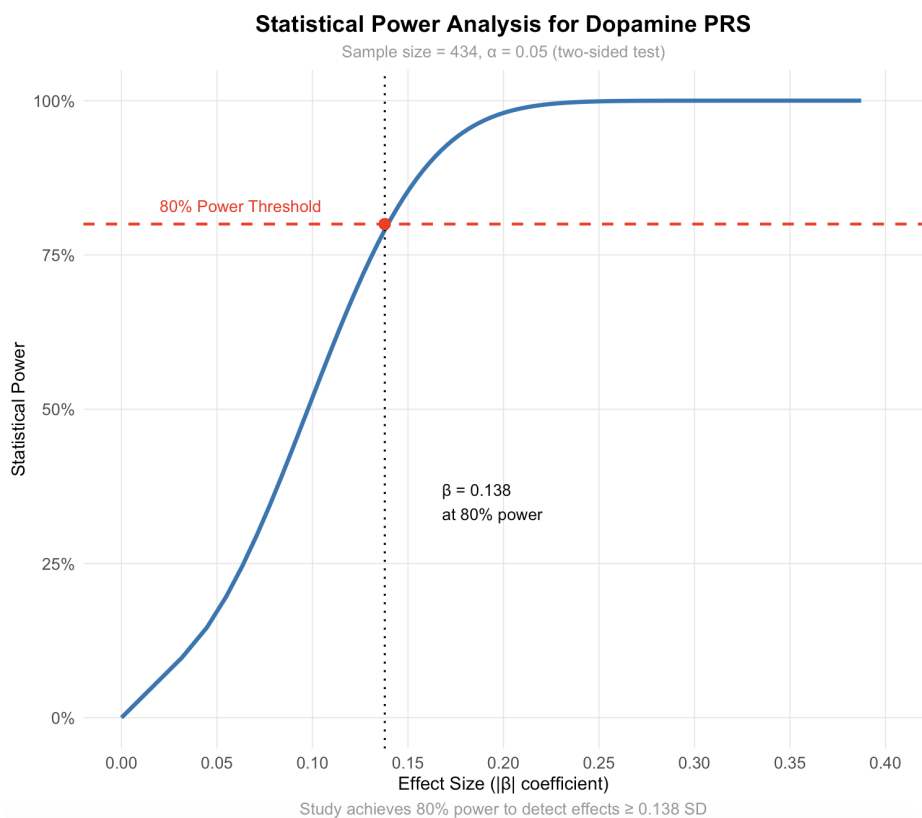
Consistent with all previous analyses, gene-based tests for fluid intelligence, episodic memory, and vocabulary intercepts yielded no significant associations after Bonferroni correction. The consistent null findings across all cognitive outcomes suggest that dopaminergic contributions to cognitive performance are not driven by detectable gene-level effects captured by this method. Complete results for secondary intercepts are in Appendix A8.

4.4 Dopamine Polygenic Risk Score Analysis

4.4.1 Statistical Power for Polygenic Score Detection

To test for cumulative pathway effects, a dopamine polygenic risk score (dPRS) was constructed by summing alleles across all 957 quality-controlled SNPs from the nine candidate genes. As a single-hypothesis test, this approach had greater statistical power than the single-variant analyses, achieving 80% power to detect a standardized effect size of $|\beta| \geq 0.14$ (Figure 10).

Figure 10. Power curve for dopamine polygenic risk-score (dPRS) association (N=434, $\alpha = 0.05$, two-sided).



Statistical power plotted against the standardized regression coefficient ($|\beta|$) for the dPRS. The horizontal line indicates the 80% power threshold, which corresponds to an effect size of $|\beta| \approx 0.14$ SD.

4.4.2 Dopamine Polygenic Risk Score Associations with Cognitive Decline Rates and Intercepts

No significant associations emerged between the dPRS and any cognitive measure, for either decline rates or performance levels at age 70 (Table 8). For decline rates, the strongest non-significant association was for processing speed ($\beta = -0.119$, $p = 0.257$). All confidence intervals included zero, mirroring the null results from the single-variant and gene-based analyses.

Table 8. Dopamine polygenic risk score associations with cognitive decline rates and performance at age 70.

Cognitive Domain	Analysis Type	Cognitive Decline Rates (Slopes)				Cognitive Performance at Age 70 (Intercepts)			
		β	SE	95% CI	P-value	β	SE	95% CI	P-value
Processing Speed	Primary Analysis	-0.119	0.105	(-0.324, 0.086)	0.257	-0.049	0.068	(-0.182, 0.084)	0.470
Fluid Intelligence	Secondary Analysis	-0.117	0.080	(-0.274, 0.041)	0.148	-0.066	0.067	(-0.198, 0.065)	0.325
Visuospatial Memory	Secondary Analysis	-0.106	0.077	(-0.258, 0.045)	0.170	-0.032	0.073	(-0.176, 0.111)	0.659
Episodic Memory	Secondary Analysis	0.022	0.082	(-0.139, 0.183)	0.787	-0.061	0.062	(-0.184, 0.061)	0.327

Abbreviations: CI, confidence interval; SE, standard error.

Association results for the standardised dPRS across cognitive decline rates (slopes) and performance at age 70 (intercepts).

4.5 Exploratory Pathway Component Analysis

4.5.1 Component 1: Genetic Associations with Neuropathology

Neuropathological Markers (n=116)

Genetic associations with post-mortem neuropathological markers were tested in 116 participants using basic covariates due to systematic clinical data missingness (Appendices A9-A10). Model diagnostics revealed unstable population stratification control with poor genomic inflation factor calibration: Braak stage ($\lambda = 0.929$), Thal phase ($\lambda = 0.538$), CAA score ($\lambda = 1.319$), α -synuclein ($\lambda = 2.712$), and TDP-43 ($\lambda = 0.443$). Statistical power was severely limited (<6% for $\beta = 0.10-0.20$), achieving adequate power (>50%) only for biologically implausible large effects ($\beta \geq 0.40$).

No SNP associations with neuropathology outcomes survived correction. The leading nominal signal was Braak stage (rs4819846, $p = 0.0005$), non-significant after correction ($q = 0.0825$). Top signals (Tables 9-10) showed large but imprecise estimates with wide confidence intervals.

Table 9. Top genetic associations with continuous neuropathology outcomes.

Chr	SNP ID	Gene	Allele	Effect			SE	L95	U95	Raw P-value	P_bonf	q (FDR)
				A2	EAF	β (SD)						
Braak Stage												
22	rs4819846	COMT	G	T	0.2818	-1.6010	0.4373	-2.4581	-0.7439	0.0005	0.4383	0.0825
22	rs5748465	COMT	A	G	0.2818	-1.6010	0.4373	-2.4581	-0.7439	0.0005	0.4383	0.0825
22	rs1878	COMT	A	G	0.2818	-1.6010	0.4373	-2.4581	-0.7439	0.0005	0.4383	0.0825
Thal Phase												
7	rs149494373	DDC	C	G	0.0748	-1.5610	0.6950	-2.9232	-0.1988	0.0277	1.0000	0.9834
7	rs2242041	DDC	G	C	0.0748	-1.5610	0.6950	-2.9232	-0.1988	0.0277	1.0000	0.9834
3	rs9825563	DRD3	G	A	0.3276	2.1800	0.9918	0.2361	4.1239	0.0307	1.0000	0.9834
CAA Score												
22	rs4646312	COMT	C	T	0.3545	0.7312	0.2912	0.1605	1.3019	0.0141	1.0000	0.8075
5	rs28363151	DAT1	A	G	0.0796	0.8267	0.3335	0.1731	1.4803	0.0153	1.0000	0.8075
9	rs4531	DBH	T	G	0.0556	1.2000	0.4890	0.2416	2.1584	0.0165	1.0000	0.8075

Abbreviations: A2, other allele; EAF, effect allele frequency; β (SD), effect size in standard deviation units; SE, standard error; L95/U95, 95% confidence interval; P_bonf, Bonferroni-corrected p-value; q(FDR), false discovery rate.

Top three SNP associations for Braak stage, Thal phase, and CAA score in the post-mortem subset ($n=116$), ranked by uncorrected p-value.

Table 10. Top genetic associations with binary neuropathology outcomes.

Chr	SNP ID	Gene	Effect		A2	EAF	OR	95% CI (OR)	Raw P-value		
			Allele	A2					P_bonf	q (FDR)	
α-Synuclein											
5	rs2975292	DAT1	C	G	0.3142	0.0604	(0.008, 0.485)	0.0083	1	0.3330	
5	rs10052016	DAT1	G	A	0.2812	3.7600	(1.396, 10.131)	0.0088	1	0.3330	
11	rs4436578	DRD2	C	T	0.0857	5.7100	(1.542, 21.138)	0.0091	1	0.3330	
TDP-43											
9	rs13284520	DBH	C	A	0.1481	0.0940	(0.015, 0.58)	0.0109	1	0.9886	
9	rs3025385	DBH	T	C	0.1481	0.0940	(0.015, 0.58)	0.0109	1	0.9886	
9	rs3025386	DBH	C	T	0.1481	0.0940	(0.015, 0.58)	0.0109	1	0.9886	

Abbreviations: A2, other allele; EAF, effect allele frequency; OR, odds ratio; 95% CI (OR), 95% confidence interval for the odds ratio; P_bonf, Bonferroni-corrected p-value; q(FDR), false discovery rate.

Top three SNP associations for α-synuclein and TDP-43 presence, ranked by uncorrected p-value.

Synaptic Density Markers n= 50

Synaptic density associations were examined across four cortical regions in 50 participants (Appendices A11-A12). Models met multicollinearity assumptions (max VIF = 4.07) but showed unstable population stratification with inflated genomic factors: frontal cortex ($\lambda = 1.535$), hippocampus ($\lambda = 1.710$), parietal cortex ($\lambda = 1.441$), occipital cortex ($\lambda = 1.370$). Power was adequate (45–59%) only for large effects ($R^2 = 0.15$ –0.20).

No associations survived correction. The strongest nominal signal was hippocampal rs1807066 ($p = 0.0002$), non-significant after correction ($p = 0.2056$). Wide confidence intervals confirmed high statistical uncertainty (Table 11).

Table 11. Top genetic associations with synaptic density markers by brain region.

Chr	SNP ID	Gene	Effect		A2	EAF	β (SD)	SE	L95	U95	Raw P-		
			Allele	A2							value	P_bonf	q (FDR)
Frontal													
5	rs72715526	DAT1	T	A	0.2021	-0.0092	0.0033	-0.0157	-0.0026	0.0149	1.0000	0.3586	
5	rs8179029	DAT1	T	C	0.2021	-0.0092	0.0033	-0.0157	-0.0026	0.0149	1.0000	0.3586	
11	rs7131056	DRD2	A	C	0.3958	0.0068	0.0027	0.0015	0.0121	0.0227	1.0000	0.4146	
Hippocampus													
7	rs1807066	DDC	T	C	0.1915	0.0315	0.0065	0.0188	0.0443	0.0002	0.2056	0.2807	
7	rs11768267	DDC	G	A	0.4362	0.0297	0.0068	0.0164	0.0430	0.0006	0.5281	0.2807	
7	rs11575534	DDC	G	T	0.4362	0.0297	0.0068	0.0164	0.0430	0.0006	0.5281	0.2807	
Parietal													
22	rs3788322	COMT	T	C	0.3854	-0.0113	0.0031	-0.0173	-0.0053	0.0020	1.0000	0.2807	
22	rs5748501	COMT	C	G	0.3854	-0.0113	0.0031	-0.0173	-0.0053	0.0020	1.0000	0.2807	
22	rs5748502	COMT	C	T	0.3854	-0.0113	0.0031	-0.0173	-0.0053	0.0020	1.0000	0.2807	
Occipital													
5	rs72715526	DAT1	T	A	0.2021	-0.0132	0.0034	-0.0198	-0.0065	0.0016	1.0000	0.2807	
5	rs8179029	DAT1	T	C	0.2021	-0.0132	0.0034	-0.0198	-0.0065	0.0016	1.0000	0.2807	
5	rs28363115	DAT1	T	C	0.2083	-0.0124	0.0033	-0.0190	-0.0058	0.0019	1.0000	0.2807	

Abbreviations: A2, other allele; EAF, effect allele frequency; β (SD), effect size in standard deviation units; SE, standard error; L95/U95, 95% confidence interval; P_bonf, Bonferroni-corrected p-value; q(FDR), false discovery rate.

Top three SNP associations for synaptic density in four cortical regions from the exploratory post-mortem subset ($n=50$), ranked by uncorrected p-value.

4.5.2 Component 2: Neuropathology Associations with Cognitive Trajectories

In the neuropathology subset ($n=116$), models met assumptions (max VIF < 2.50) with adequate power (>80%) only for substantial effects ($\beta \geq 0.25$ SD). No markers were significantly associated with processing speed after FDR correction (all $q = 0.966$). The strongest association was Braak stage with decline ($\beta = -0.079$, $p = 0.261$). Models explained ~10% variance in decline rates, 21% in performance levels (Table 12).

Table 12. Neuropathology Marker Associations with Processing Speed Trajectories.

Neuropathology Marker	Analysis Type	β (SD)	95% CI	Raw P-value	P_bonf	q (FDR)	R²
Braak Stage	Slopes	-0.079	(-0.216, 0.058)	0.261	1	0.966	0.107
	Intercepts	-0.012	(-0.108, 0.085)	0.813	1	0.966	0.214
Thal Phase	Slopes	-0.039	(-0.194, 0.115)	0.620	1	0.966	0.099
	Intercepts	-0.004	(-0.113, 0.105)	0.946	1	0.966	0.214
CAA Score	Slopes	-0.012	(-0.242, 0.217)	0.916	1	0.966	0.096
	Intercepts	0.076	(-0.084, 0.237)	0.353	1	0.966	0.220
α -Synuclein	Slopes	0.103	(-0.611, 0.817)	0.778	1	0.966	0.097
	Intercepts	0.108	(-0.394, 0.609)	0.674	1	0.966	0.215
TDP-43	Slopes	0.013	(-0.59, 0.616)	0.966	1	0.966	0.096
	Intercepts	0.065	(-0.358, 0.489)	0.763	1	0.966	0.214

Abbreviations: β (SD), standardized effect size; CI, confidence interval; P_bonf, Bonferroni-corrected p-value; q(FDR), false discovery rate; R², proportion of variance explained

Associations between five neuropathological markers and processing speed trajectories (slopes and intercepts).

Synaptic Density Associations with Cognitive Trajectories

In the subset (n=50), models met assumptions (max VIF < 5.0) but power was severely limited, adequate (>80%) only for very large effects ($\beta \geq 0.40$ SD). No associations survived correction (all FDR q > 0.88). The strongest finding was hippocampal density with decline ($\beta = -27.66$, p = 0.282) with exceptionally wide confidence intervals [-77.34, 22.02]. Model R² ranged 5.0-21.7% (Table 13).

Table 13. Synaptic Density Associations with Processing Speed Trajectories.

Brain Region	Analysis Type	β (SD)	95% CI	Raw P-value	P_bonf	q (FDR)	R ²
Frontal	Slopes	3.296	(-53.028, 59.62)	0.909	1	0.974	0.050
	Intercepts	8.851	(-27.462, 45.164)	0.636	1	0.947	0.214
Hippocampus	Slopes	-27.662	(-77.342, 22.018)	0.282	1	0.881	0.079
	Intercepts	-9.792	(-42.263, 22.678)	0.558	1	0.947	0.217
Parietal	Slopes	-6.228	(-65.053, 52.598)	0.837	1	0.974	0.051
	Intercepts	11.557	(-26.32, 49.433)	0.553	1	0.947	0.217
Occipital	Slopes	3.081	(-47.953, 54.114)	0.906	1	0.974	0.050
	Intercepts	9.585	(-23.275, 42.445)	0.571	1	0.947	0.216

Abbreviations: β (SD), standardized effect size; CI, confidence interval; P_bonf, Bonferroni-corrected p-value; q(FDR), false discovery rate; R², proportion of variance explained

Associations between synaptic density in four cortical brain regions and processing speed trajectories (slopes and intercepts).

5. Discussion

5.1 Reconciling Null Genetic Findings with Dopamine Neurobiology

A Comprehensive Null Result Across Multiple Analytical Approaches

This investigation aimed to determine if common dopaminergic variation modulates processing speed decline. After a comprehensive analysis of 957 variants across nine key genes, the study yielded a striking absence of statistically significant associations. This null finding persisted across all three analytical tiers, as single-variant, gene-based, and polygenic risk score analyses all failed to show significant associations. For processing speed decline, the strongest nominal signals, such as a variant in DBH (rs3025383, p=0.008) and the gene-based signal for DRD2 (p=0.222), failed to survive multiple testing correction. This pervasive null pattern extended to all secondary cognitive domains and the exploratory post-mortem analyses. These findings are consistent with the contemporary view that complex traits are highly polygenic, where

individual gene effects are too small for detection in candidate-gene studies. This pattern aligns with findings like Border et al. (2019), who demonstrated that candidate-gene associations often fail to replicate in large-scale studies, suggesting such approaches may be prone to false positives. However, our limited sample size restricts power to detect very small effects, so larger studies would be needed to definitively exclude subtle genetic influences.

The Disconnect with Established Neurobiology

These findings prompt a reconsideration of the genetic drivers of cognitive aging. This study's robust null result creates a significant disconnect from decades of research establishing dopamine's critical role in cognition. The "correlative triad" framework and extensive molecular imaging data provide a powerful biological rationale for expecting an association. This presents the central question for this discussion: why does this strong, system-level neurobiological relationship not translate into detectable effects from common genetic variants? The answer likely lies in a combination of complex biological realities and this study's specific methodological scope.

Interpreting the Null Finding as Meaningful Scientific Evidence

Crucially, careful consideration of this study's statistical power allows these null results to be interpreted as meaningful scientific evidence. With 80% power to detect single-variant effects of $\beta \geq 0.24$ SD per allele, the analysis could reliably identify any variant explaining approximately 5.3% or more of the variance in processing speed decline. The comprehensive absence of such signals supports the absence of this class of genetic effect, rather than reflecting a simple failure to detect existing associations. Furthermore, the polygenic risk score analysis, with enhanced power to detect cumulative effects of $|\beta| \geq 0.14$, strengthens this conclusion by demonstrating that even aggregated pathway-wide variation lacks detectable influence.

Methodological Rigor and the Importance of Deep Phenotyping

The credibility of these conclusions is supported by the study's robust design. A 12-year longitudinal framework provided dynamic phenotypes of cognitive change, while a multi-tiered analytical strategy (single-variant, gene-based, and polygenic tests) ensured the null finding was not a methodological artifact.

A key methodological insight emerged from a sensitivity analysis comparing the primary, fully-adjusted model ($N=434$) with a larger, less-adjusted model ($N=1,179$). The resulting genomic deflation (genomic inflation factor = 0.813) in the larger sample

provided direct evidence for the importance of deep phenotyping: the precise and comprehensive analysis of phenotypic variables needed to correctly interpret genomic data (Robinson, 2012). This deflation likely reflects a downward bias caused by omitting important, heritable confounders (Sul et al., 2018; Tu et al., 2025), specifically key clinical covariates like blood pressure and BMI that were systematically missing in the larger sample. This finding provides a powerful, data-driven justification for prioritizing the smaller, more robustly controlled sample, underscoring that for complex aging phenotypes, the quality of phenotypic data may be more critical for valid causal inference than sheer sample size.

5.2 Interpretation of Null Genetic Findings

A primary set of explanations is rooted in the immense complexity of the genetic architecture underlying cognitive traits, which a candidate-gene approach may be too narrowly focused to capture.

The Polygenic Architecture of Cognitive Aging

The null findings are likely explained by extreme polygenicity, a model where cognitive differences arise from the cumulative impact of many genetic variants, each with a very small effect. For instance, a large-scale meta-analysis found that top-associated SNPs for cognitive function individually accounted for only ~0.1% of the variance (Trampush et al., 2017). Within this framework, the failure to detect single-variant associations does not mean dopaminergic genes are uninvolved, but rather that their individual effects were too subtle for the available statistical power.

Similarly, the null result for the dopamine polygenic risk score (dPRS) is consistent with this model. While common variants in total account for substantial heritability in cognitive function, estimated at around 21.5% (Trampush et al., 2017), this influence is distributed thinly across the entire genome. A dPRS focused on only nine candidate genes therefore captures just a fraction of the total genetic architecture, reinforcing the conclusion that any contribution from these specific genes was too subtle for detection in this cohort.

Unassessed Genetic Variation: Rare and Structural Variants

The study's focus on common SNPs is another limitation, as it leaves other important classes of variation unassessed. Rare variants ($MAF < 1\%$), which can have a greater phenotypic influence due to negative selection, may explain some of the "missing heritability" not captured in this analysis (Zeggini and Morris, 2015; Li et al., 2013).

Similarly, structural variants (SVs) like deletions and variable number tandem repeats (VNTRs) can profoundly impact gene function but are poorly captured by SNP arrays, which may fail to detect or can misclassify them (Rahbari et al., 2024). This limitation is particularly relevant here due to the exclusion of two well-studied functional VNTRs in SLC6A3 and DRD4. The DRD4 gene was not assayed, and while SLC6A3 was included, its functional VNTR was not analyzed. The omission is significant, as these specific VNTRs are linked by decades of research to dopamine signaling, with meta-analyses confirming associations with ADHD and dopamine transporter availability (Rafikova et al., 2021; Grünblatt et al., 2019; Li et al., 2006).

Dynamic Gene Regulation and Epigenetics

Beyond the static DNA sequence, a further explanation for the null findings lies in dynamic gene regulation. A key limitation of this study is its reliance on a single, static genetic measurement to model a dynamic process like cognitive change over 12 years.

The epigenome, a layer of modifications such as DNA methylation, dynamically regulates gene expression in response to the environment, and its age-related alterations are considered a core driver of cognitive decline (An et al., 2025). The true drivers of cognitive change may therefore be this age-related dysregulation, rather than the inherited variants themselves. Studies confirm that DNA methylation patterns in brain tissue change with age, which is linked to cognitive impairment (Harman & Martín, 2019). This means two individuals with an identical COMT genotype could have different cognitive trajectories due to different methylation of the COMT promoter over time. A genetic model that does not account for this dynamic layer averages across these distinct states, which could obscure a true relationship and explain the null result.

Conditional Genetic Effects: Gene-Environment Interactions

A final explanation for the null findings is Gene-Environment interaction (GxE), where a variant's effect is conditional on environmental exposures. Such interactions can explain null results, as a variant with opposing effects in different contexts can average to zero in a statistical model testing only for main effects (Blair et al., 2015). The

COMT Val158Met polymorphism is a canonical example; its effect on cognition is governed by an inverted U-shaped relationship between dopamine and prefrontal function (Dickinson and Elvevåg, 2009).

This is highly relevant as this dissertation tested only for main effects. The null COMT finding could therefore be a direct result of a GxE, where the allele's effects differ based

on an unmeasured factor like cognitive reserve. Given the study's limited power, the null result could also simply reflect an inability to detect a small main effect. The finding should therefore not be interpreted as definitive evidence against COMT's role in cognitive aging. Instead, it presents a plausible alternative hypothesis that requires future testing in larger cohorts with sufficient power to investigate such complex interactions.

5.3 Future Directions

This study's null findings and methodological scope provide a clear roadmap for future research. The path forward requires moving beyond the limitations of the candidate-gene approach by enhancing statistical power, broadening genetic coverage, and increasing demographic diversity.

Enhancing Statistical Power and Genetic Coverage

To overcome the primary constraint of statistical power and detect the subtle effects characteristic of a highly polygenic trait, future studies must utilize substantially larger samples. This is particularly critical for rare outcomes, such as the post-mortem analyses in this study, which highlight the need for larger, deeply phenotyped brain bank resources.

In parallel, future work must employ whole-genome sequencing (WGS) to capture the full spectrum of genetic variation. WGS would provide comprehensive coverage of rare variants and structural polymorphisms, such as the functional VNTRs in SLC6A3 and DRD4 that were unassessed in this analysis. This approach would also resolve inconsistent SNP coverage across genes, thereby improving the power and validity of gene-based tests.

Broadening Generalizability through Cohort Diversity

The cohort's European ancestry limits the generalizability of these findings, as allele frequencies and linkage disequilibrium patterns differ substantially across global populations. A crucial future direction is therefore a commitment to recruiting and analyzing genetically diverse populations to ensure that findings are robust and transferable to other ancestral groups.

Beyond Static Genes and Single Pathways

To better model the dynamic nature of aging, future research must move beyond static genetic data. This requires longitudinal methods that capture change over time, such as Epigenome-Wide Association Studies (EWAS) to map age-related epigenetic drift and analyses that test for gene-environment interactions.

Similarly, research should expand from a single-pathway focus to an integrative, systems-biology approach, as the dopamine system is modulated by complex neurobiological networks. Future work should investigate key interactions with brain-derived neurotrophic factor (BDNF), a critical regulator of synaptic plasticity (Woo & Lu, 2009; Yang et al., 2020), and the glutamatergic system, whose balance with dopamine is essential for executive functions (Lorenz et al., 2015). Other important modulators include the circadian system (Maiese, 2021) and adjacent regulatory loci. For instance, the Taq1A polymorphism in the nearby ANKK1 gene is associated with reduced D2/3 receptor binding, illustrating that important variants may lie outside canonical gene boundaries (Savitz et al., 2013).

A Multi-Modal Framework for Future Research

Ultimately, a truly mechanistic understanding requires integrating these advances into a multi-modal framework. The ideal future study would combine comprehensive genetics (WGS), longitudinal deep phenotyping, and in-vivo brain imaging (e.g., dopamine PET) within the same large, diverse cohort. This design would enable powerful causal inference methods, such as Mendelian randomization, to formally test the complex pathways from genetic variation through brain biology to cognitive decline.

6. Conclusion

This study provides evidence that common dopaminergic variants do not influence processing speed decline above our detection threshold in cognitive aging. Despite comprehensive pathway coverage across 957 variants and adequate power to detect meaningful effects, no associations survived correction across multiple analytical approaches.

These null findings meaningfully refine our understanding of the dopamine-cognition relationship. While neuroimaging consistently demonstrates that dopamine system integrity predicts cognitive performance, this relationship appears disconnected from inherited common genetic variation. This disconnect suggests that dopaminergic

influences on cognitive aging operate through mechanisms beyond common variants, potentially rare variants, dynamic epigenetic regulation, or gene-environment interactions that vary across individuals and time.

The results support the highly polygenic architecture of cognitive traits and demonstrate how systematic null findings advance theoretical understanding. The established correlative triad framework requires extension beyond static genetic models toward investigations integrating neuroimaging, genomics, and dynamic regulatory mechanisms to capture the complex pathways linking dopamine biology to cognitive aging outcomes.

7. References

- Aichele, S., Rabbitt, P.M.A. and Ghisletta, P. (2016) 'Think Fast, Feel Fine, Live Long: A 29-Year Study of Cognition, Health and Survival in Middle-Aged and Older Adults', *Psychological Science*, 27(4), pp. 518–529.
- 'Alphabet Coding Task 15' (1984). Savage, R.D: Murdoch University.
- An, Y. et al. (2025) 'Epigenetic Regulation of Aging and its Rejuvenation', *MedComm*, 6(9), p. e70369. Available at: <https://doi.org/10.1002/mco2.70369>.
- Angevaren, M. et al. (2008) 'Physical activity and enhanced fitness to improve cognitive function in older people without known cognitive impairment', in The Cochrane Collaboration (ed.) *Cochrane Database of Systematic Reviews*. Chichester, UK: John Wiley & Sons, Ltd, p. CD005381.pub3. Available at: <https://doi.org/10.1002/14651858.CD005381.pub3>.
- Anstey, K. et al. (2005) 'Cognitive, sensory and physical factors enabling driving safety in older adults', *Clinical Psychology Review*, 25(1), pp. 45–65. Available at: <https://doi.org/10.1016/j.cpr.2004.07.008>.
- Anstey, K.J. et al. (2007) 'Smoking as a Risk Factor for Dementia and Cognitive Decline: A Meta-Analysis of Prospective Studies', *American Journal of Epidemiology*, 166(4), pp. 367–378. Available at: <https://doi.org/10.1093/aje/kwm116>.
- Bäckman, L. et al. (2000) 'Age-related cognitive deficits mediated by changes in the striatal dopamine system', *American Journal of Psychiatry*, 157(4), pp. 635–637. Available at: <https://doi.org/10.1176/ajp.157.4.635>.
- Bäckman, L. et al. (2006) 'The correlative triad among aging, dopamine, and cognition: Current status and future prospects', *Neuroscience & Biobehavioral Reviews*, 30(6), pp. 791–807. Available at: <https://doi.org/10.1016/j.neubiorev.2006.06.005>.
- Baddeley, A., Emslie, H. and Nimmo-Smith, I. (1992) *Speed and Capacity of Language Processing Test (SCOLP) Manual*. Bury St Edmunds: Thames Valley Test Company.
- Barnett, J.H., Scorials, L. and Munafò, M.R. (2008) 'Meta-Analysis of the Cognitive Effects of the Catechol-O-Methyltransferase Gene Val158/108Met Polymorphism', *Biological Psychiatry*, 64(2), pp. 137–144. Available at: <https://doi.org/10.1016/j.biopsych.2008.01.005>.

- Baron, R.M. and Kenny, D.A. (1986) 'The moderator-mediator variable distinction in social psychological research: conceptual, strategic, and statistical considerations', *Journal of Personality and Social Psychology*, 51(6), pp. 1173–1182.
- Beck, A.T. et al. (1961) 'An inventory for measuring depression', *Archives of General Psychiatry*, 4, pp. 561–571. Available at:
<https://doi.org/10.1001/archpsyc.1961.01710120031004>.
- Beeri, M.S. et al. (2022) 'Stability in BMI over time is associated with a better cognitive trajectory in older adults', *Alzheimer's & Dementia*, 18(11), pp. 2131–2139. Available at:
<https://doi.org/10.1002/alz.12525>.
- Berry, A.S. et al. (2016) 'Aging affects dopaminergic neural mechanisms of cognitive flexibility', *Journal of Neuroscience*, 36(50), pp. 12559–12569. Available at:
<https://doi.org/10.1523/JNEUROSCI.0626-16.2016>.
- Blair, C. et al. (2015) 'Catechol- O -methyltransferase Val158met polymorphism interacts with early experience to predict executive functions in early childhood', *Developmental Psychobiology*, 57(7), pp. 833–841. Available at:
<https://doi.org/10.1002/dev.21332>.
- Border, R. et al. (2019) 'No support for historical candidate gene or candidate gene-by-interaction hypotheses for major depression across multiple large samples', *American Journal of Psychiatry*, 176(5), pp. 376–387.
- Braak, H. et al. (2006) 'Staging of Alzheimer disease-associated neurofibrillary pathology using paraffin sections and immunocytochemistry', *Acta Neuropathologica*, 112(4), pp. 389–404.
- Cattell, R.B. and Cattell, A.K.S. (1960) *Handbook for the Culture Fair Intelligence Test, Scale 3*. Champaign, IL: Institute for Personality and Ability Testing.
- Chang, C.C. et al. (2015a) 'Second-generation PLINK: rising to the challenge of larger and richer datasets', *Gigascience*, 4(1), pp. s13742-015-0047-8. Available at:
<https://doi.org/10.1186/s13742-015-0047-8>.
- Chang, C.C. et al. (2015b) 'Second-generation PLINK: rising to the challenge of larger and richer datasets', *Gigascience*, 4(1), pp. s13742-015-0047-8. Available at:
<https://doi.org/10.1186/s13742-015-0047-8>.
- Cools, R. and D'Esposito, M. (2011) 'Inverted-U-shaped dopamine actions on human working memory and cognitive control', *Biological Psychiatry*, 69(12), pp. 113–125. Available at: <https://doi.org/10.1016/j.biopsych.2011.03.028>.

Davies, G. et al. (2016) 'Genome-wide association study of cognitive functions and educational attainment in UK Biobank (N = 112 151)", Molecular Psychiatry, 21(6), pp. 758–767. Available at: <https://doi.org/10.1038/mp.2016.45>.

Davis, J.C. (2017) 'Slow processing speed predicts falls in older adults with a falls history: A 1-year prospective study", Journal of the American Geriatrics Society, 65(5), pp. 916–923.

De Leeuw, C.A. et al. (2015) 'MAGMA: Generalized Gene-Set Analysis of GWAS Data', PLOS Computational Biology. Edited by H. Tang, 11(4), p. e1004219. Available at: <https://doi.org/10.1371/journal.pcbi.1004219>.

Dickinson, D. and Elvevåg, B. (2009) 'Genes, cognition and brain through a COMT lens', Neuroscience, 164(1), pp. 72–87. Available at: <https://doi.org/10.1016/j.neuroscience.2009.05.014>.

Didikoglu, A. et al. (2022) 'Associations between chronotype and employment status in a longitudinal study of an elderly population', Chronobiology International, 39(8), pp. 1118–1131. Available at: <https://doi.org/10.1080/07420528.2022.2071158>.

D.P., E., P.D., K. and C.E., H. (2016) 'Common variation in the DOPA decarboxylase (DDC) gene and human striatal DDC activity in vivo", Neuropsychopharmacology, 41(11), pp. 2303–2308. Available at: <https://doi.org/10.1038/npp.2016.31>.

Dyck, C.H. et al. (2008) 'Striatal dopamine transporters correlate with simple reaction time in elderly subjects", Neurobiology of Aging, 29(8), pp. 1237–1246. Available at: <https://doi.org/10.1016/j.neurobiolaging.2007.02.012>.

Edwards, J.D. et al. (2017) 'Speed of processing training results in lower risk of dementia", Alzheimer's & Dementia: Translational Research & Clinical Interventions, 3(4), pp. 603–611. Available at: <https://doi.org/10.1016/j.trci.2017.09.002>.

Eisenberg, D.P. et al. (2016) 'Common Variation in the DOPA Decarboxylase (DDC) Gene and Human Striatal DDC Activity In Vivo', Neuropsychopharmacology, 41(9), pp. 2303–2308. Available at: <https://doi.org/10.1038/npp.2016.31>.

Erixon-Lindroth, N. et al. (2005) 'The role of the striatal dopamine transporter in cognitive aging", Psychiatry Research: Neuroimaging, 138(1), pp. 1–12. Available at: <https://doi.org/10.1016/j.pscychresns.2004.09.005>.

Gkotzamanis, V. et al. (2021) 'Determinants of Processing Speed Trajectories among Middle Aged or Older Adults, and Their Association with Chronic Illnesses: The

English Longitudinal Study of Aging', *Life*, 11(4), p. 357. Available at:
<https://doi.org/10.3390/life11040357>.

Grünblatt, E. et al. (2019) 'Association study and a systematic meta-analysis of the VNTR polymorphism in the 3'-UTR of dopamine transporter gene and attention-deficit hyperactivity disorder', *Journal of Neural Transmission*, 126(4), pp. 517–529. Available at: <https://doi.org/10.1007/s00702-019-01998-x>.

Harman, M.F. and Martín, M.G. (2020) 'Epigenetic mechanisms related to cognitive decline during aging', *Journal of Neuroscience Research*, 98(2), pp. 234–246. Available at: <https://doi.org/10.1002/jnr.24436>.

Heim, A.W. (1970) A.H.4 Group Test of General Intelligence: Manual. revised. Windsor: NFER-Nelson.

Heinz, A. et al. (2000) 'Genotype influences in vivo dopamine transporter availability in human striatum', *Neuropsychopharmacology*, 22(2), pp. 133–139. Available at: [https://doi.org/10.1016/S0893-133X\(99\)00099-8](https://doi.org/10.1016/S0893-133X(99)00099-8).

Hülür, G. et al. (2016) 'Cognitive Aging in the Seattle Longitudinal Study: Within-Person Associations of Primary Mental Abilities with Psychomotor Speed and Cognitive Flexibility', *Journal of Intelligence*, 4(3), p. 12. Available at: <https://doi.org/10.3390/intelligence4030012>.

Hupfeld, K.E., Vaillancourt, D.E. and Seidler, R.D. (2018) 'Genetic markers of dopaminergic transmission predict performance for older males but not females', *Neurobiology of Aging*, 66, p. 180 11-180 21. Available at: <https://doi.org/10.1016/j.neurobiolaging.2018.02.018>.

Ibrahim-Verbaas, C.A., Bressler, J. and Debette, S. (2016) 'GWAS for executive function and processing speed suggests involvement of the CADM2 gene', *Molecular Psychiatry*, 21(6), pp. 781–789.

Imai, K., Keele, L. and Yamamoto, T. (2010) 'Identification, inference and sensitivity analysis for causal mediation effects', *Statistical Science*, 25(1), pp. 51–71.

J.H., B., L., S. and M.R, M. (2008) 'Meta-analysis of the cognitive effects of the catechol-O-methyltransferase gene Val158/108Met polymorphism', *Biological Psychiatry*, 64(2), pp. 137–144. Available at: <https://doi.org/10.1016/j.biopsych.2008.01.005>.

Jiang, M. et al. (2024) 'Association of sleep quality with cognitive dysfunction in middle-aged and elderly adults: a cross-sectional study in China', *Frontiers in Aging Neuroscience*, 16, p. 1417349. Available at: <https://doi.org/10.3389/fnagi.2024.1417349>.

Juárez Olguín, H. et al. (2016) 'The Role of Dopamine and Its Dysfunction as a Consequence of Oxidative Stress', *Oxidative Medicine and Cellular Longevity*. Edited by A.-L. Bulteau, 2016(1), p. 9730467. Available at: <https://doi.org/10.1155/2016/9730467>.

Kandlur, A., Satyamoorthy, K. and Gangadharan, G. (2020) 'Oxidative Stress in Cognitive and Epigenetic Aging: A Retrospective Glance', *Frontiers in Molecular Neuroscience*, 13, p. 41. Available at: <https://doi.org/10.3389/fnmol.2020.00041>.

Karalija, N. et al. (2024) 'Longitudinal support for the correlative triad among aging, dopamine D2-like receptor loss, and memory decline', *Neurobiology of Aging*, 133, pp. 54–64. Available at: <https://doi.org/10.1016/j.neurobiolaging.2024.02.001>.

Karrer, T.M. et al. (eds) (2017) 'Reduced dopamine receptors and transporters but not synthesis capacity in normal aging adults: a meta-analysis', *Neurobiology of Aging*, 57, pp. 36–46. Available at: <https://doi.org/10.1016/j.neurobiolaging.2017.05.006>.

Kochan, N.A., Bunce, D. and Pont, S. (2016) 'Reaction time measures predict incident dementia in community-living older adults: the Sydney Memory and Ageing Study', *American Journal of Geriatric Psychiatry*, 24(3), pp. 221–231. Available at: <https://doi.org/10.1016/j.jagp.2015.12.005>.

Kovacs, G.G. (2016) 'Guidelines for the assessment of α-synuclein pathology and TDP-43 inclusions in neurodegenerative diseases', *Neuropathology and Applied Neurobiology*, 42(6), pp. 497–527.

Lane, H.-Y. et al. (2008) 'Prefrontal executive function and D1, D3, 5-HT2A and 5-HT6 receptor gene variations in healthy adults', *Journal of Psychiatry & Neuroscience*, 33(1), pp. 47–53.

Le Moine, C. and Bloch, B. (1996) 'Expression of D3 dopamine receptor in peptidergic neurons of the nucleus accumbens: comparison with D1 and D2 dopamine receptors', *Neuroscience*, 73(1), pp. 131–143. Available at: [https://doi.org/10.1016/0306-4522\(96\)00037-5](https://doi.org/10.1016/0306-4522(96)00037-5).

Li, B., Liu, D.J. and Leal, S.M. (2013) 'Identifying Rare Variants Associated with Complex Traits via Sequencing', *Current Protocols in Human Genetics*, 78(1). Available at: <https://doi.org/10.1002/0471142905.hg0126s78>.

- Li, D. et al. (2006) 'Meta-analysis shows significant association between dopamine system genes and attention deficit hyperactivity disorder (ADHD)', *Human Molecular Genetics*, 15(14), pp. 2276–2284. Available at: <https://doi.org/10.1093/hmg/ddl152>.
- Li, S.C. et al. (2013) 'Dopamine modulates attentional control of auditory perception: DARPP-32 (PPP1R1B) genotype effects on behavior and cortical evoked potentials', *Neuropsychologia*, 51(8), pp. 1649–1661.
- Liu, C.-C. et al. (2013) 'Apolipoprotein E and Alzheimer disease: risk, mechanisms and therapy', *Nature Reviews Neurology*, 9(2), pp. 106–118. Available at: <https://doi.org/10.1038/nrneurol.2012.263>.
- Lo, J.C. et al. (2016) 'Self-reported sleep duration and cognitive performance in older adults: a systematic review and meta-analysis', *Sleep Medicine*, 17, pp. 87–98. Available at: <https://doi.org/10.1016/j.sleep.2015.08.021>.
- Lorenz, R.C. et al. (2015) 'Interactions between glutamate, dopamine, and the neuronal signature of response inhibition in the human striatum', *Human Brain Mapping*, 36(10), pp. 4031–4040. Available at: <https://doi.org/10.1002/hbm.22895>.
- Lundström, K. and Turpin, M.-P. (1996) 'Proposed schizophrenia-related gene polymorphism: expression of the Ser9Gly mutant human dopamine D3 receptor with the Semliki Forest virus system', *Biochemical and Biophysical Research Communications*, 225(3), pp. 1068–1072. Available at: <https://doi.org/10.1006/bbrc.1996.1293>.
- M., H., A., L. and K., N. (2009) 'C957T polymorphism of the dopamine D2 receptor gene affects striatal DRD2 availability in vivo', *Molecular Psychiatry*, 14(4), pp. 369–371. Available at: <https://doi.org/10.1038/sj.mp.4002140>.
- MacRae, P.G., Spirduso, W.W. and Wilcox, R.E. (1988) 'Reaction time and nigrostriatal dopamine function: the effects of age and practice', *Brain Research*, 451(1-2), pp. 139–146. Available at: [https://doi.org/10.1016/0006-8993\(88\)90758-5](https://doi.org/10.1016/0006-8993(88)90758-5).
- Maiese, K. (2021) 'Cognitive Impairment and Dementia: Gaining Insight through Circadian Clock Gene Pathways', *Biomolecules*, 11(7), p. 1002. Available at: <https://doi.org/10.3390/biom11071002>.
- Makar, A.B. et al. (1975) 'Formate assay in body fluids: application in methanol poisoning', *Biochemical Medicine*, 13(2), pp. 117–126. Available at: [https://doi.org/10.1016/0006-2944\(75\)90147-7](https://doi.org/10.1016/0006-2944(75)90147-7).

Malén, T. et al. (2022) 'Atlas of type 2 dopamine receptors in the human brain: age and sex dependent variability in a large PET cohort', *NeuroImage*, 255, p. 119149. Available at: <https://doi.org/10.1016/j.neuroimage.2022.119149>.

Manuck, S.B. and McCaffery, J.M. (2014) 'Gene-Environment Interaction', *Annual Review of Psychology*, 65(1), pp. 41–70. Available at: <https://doi.org/10.1146/annurev-psych-010213-115100>.

Marks, S.M. et al. (2017) 'Tau and β-Amyloid Are Associated with Medial Temporal Lobe Structure, Function, and Memory Encoding in Normal Aging', *The Journal of Neuroscience*, 37(12), pp. 3192–3201. Available at: <https://doi.org/10.1523/JNEUROSCI.3769-16.2017>.

Meiser, J., Weindl, D. and Hiller, K. (2013) 'Complexity of dopamine metabolism', *Cell Communication and Signaling*, 11(1), p. 34. Available at: <https://doi.org/10.1186/1478-811X-11-34>.

Meyer-Lindenberg, A. et al. (2007) 'Genetic evidence implicating DARPP-32 in human frontostriatal structure, function, and cognition', *Journal of Clinical Investigation*, 117(3), pp. 672–682.

Michelhaugh, S.K. et al. (2001) 'The dopamine transporter gene (SLC6A3) variable number of tandem repeats domain enhances transcription in dopamine neurons', *Journal of Neurochemistry*, 79(5), pp. 1033–1038. Available at: <https://doi.org/10.1046/j.1471-4159.2001.00647.x>.

Montine, T.J. et al. (2012) 'National Institute on Aging-Alzheimer's Association guidelines for the neuropathologic assessment of Alzheimer's disease: a practical approach', *Acta Neuropathologica*, 123(1), pp. 1–11.

Moroi, K. and Sato, T. (1975) 'Comparison between procaine and isocarboxazid metabolism in vitro by a liver microsomal amidase-esterase', *Biochemical Pharmacology*, 24(16), pp. 1517–1521. Available at: [https://doi.org/10.1016/0006-2952\(75\)90029-5](https://doi.org/10.1016/0006-2952(75)90029-5).

Moura, C. and Vale, N. (2023) 'The Role of Dopamine in Repurposing Drugs for Oncology', *Biomedicines*, 11(7). Available at: <https://doi.org/10.3390/biomedicines11071917>.

Parasuraman, R. et al. (2005) 'Beyond heritability: neurotransmitter genes differentially modulate visuospatial attention and working memory', *Psychological Science*, 16(3), pp. 200–207. Available at: <https://doi.org/10.1111/j.0956-7976.2005.00804.x>.

- Parasuraman, R. et al. (2012) 'Dopamine beta hydroxylase genotype identifies individuals less susceptible to bias in computer-assisted decision making', PLoS One, 7(6), p. 39675. Available at: <https://doi.org/10.1371/journal.pone.0039675>.
- Pellegrino, L.D. et al. (2013) 'Depression in Cognitive Impairment', Current Psychiatry Reports, 15(9), p. 384. Available at: <https://doi.org/10.1007/s11920-013-0384-1>.
- Rabbitt, P. et al. (2004) 'Practice and drop-out effects during a 17-year longitudinal study of cognitive aging', Journal of Gerontology: Psychological Sciences, 59B(2), pp. 84–97.
- Rafikova, E. et al. (2021) 'SLC6A3 (DAT1) as a Novel Candidate Biomarker Gene for Suicidal Behavior', Genes, 12(6), p. 861. Available at: <https://doi.org/10.3390/genes12060861>.
- Rahbari, R. et al. (2024) 'Complex de novo structural variants are an underestimated cause of rare disorders'. In Review. Available at: <https://doi.org/10.21203/rs.3.rs-4197130/v1>.
- Ramsingh, N. et al. (2024) 'Poor self-rated health is associated with faster cognitive decline and greater small vessel disease in older adults with type 2 diabetes', Diabetes/Metabolism Research and Reviews, 40(1), p. e3761. Available at: <https://doi.org/10.1002/dmrr.3761>.
- Rieckmann, A. et al. (2011) 'Caudate Dopamine D1 Receptor Density Is Associated with Individual Differences in Frontoparietal Connectivity during Working Memory', The Journal of Neuroscience, 31(40), pp. 14284–14290. Available at: <https://doi.org/10.1523/JNEUROSCI.3114-11.2011>.
- Rihet, P., Fiori, M. and Combe, R. (2002) 'Dopamine and human information-processing: effects of levodopa administration on reaction time task performance', Behavioural Brain Research, 134(1-2), pp. 271–278.
- Robinson, J.L. et al. (2020) 'Enhanced associations between neuropathology and cognition in a late-life autopsy cohort after accounting for concomitant pathologies', Brain, 143(12), pp. 3873–3885.
- Robinson, P.N. (2012) 'Deep phenotyping for precision medicine', Human Mutation, 33(5), pp. 777–780. Available at: <https://doi.org/10.1002/humu.22080>.
- Sabia, S. et al. (2014) 'Alcohol consumption and cognitive decline in early old age', Neurology, 82(4), pp. 332–339. Available at: <https://doi.org/10.1212/WNL.0000000000000063>.

- Salthouse, T. (1996) 'The Processing-Speed Theory of Adult Age Differences in Cognition', *Psychological review*, 103, pp. 403-28 10 1037 0033-295 103 3 403.
- Salthouse, T.A. (1991) 'Mediation of adult age differences in cognition by reductions in working memory and speed of processing', *Psychological Science*, 2(3), pp. 179-183.
- Salthouse, T.A. (2000) 'Aging and measures of processing speed', *Biological Psychology*, 54(1-3), pp. 35-54. Available at: [https://doi.org/10.1016/S0301-0511\(00\)00052-1](https://doi.org/10.1016/S0301-0511(00)00052-1).
- Salthouse, T.A. (2009) 'When does age-related cognitive decline begin?', *Neurobiology of Aging*, 30(4), pp. 507-514. Available at: <https://doi.org/10.1016/j.neurobiolaging.2008.09.023>.
- Savitz, J. et al. (2013) 'DRD2/ANKK1 Taq1A polymorphism (rs1800497) has opposing effects on D2/3 receptor binding in healthy controls and patients with major depressive disorder', *International Journal of Neuropsychopharmacology*, 16(9), pp. 2095-2101. Available at: <https://doi.org/10.1017/S146114571300045X>.
- Schafer, J.L. (1999) 'Multiple imputation: a primer', *Statistical Methods in Medical Research*, 8(1), pp. 3-15. Available at: <https://doi.org/10.1177/096228029900800102>.
- Schaie, K.W., Willis, S.L. and Caskie, G.I.L. (2004) 'The Seattle Longitudinal Study: relationship between personality and cognition', *Aging, Neuropsychology and Cognition*, 11(2-3), pp. 304-324. Available at: <https://doi.org/10.1080/13825580490511134>.
- Seaman, K.L., Brooks, N. and Karrer, T.M. (2024) 'Longitudinal loss of dopamine D2-like receptors predicts memory decline in healthy aging', *eLife*, 13, p. 86892.
- Sul, J.H., Martin, L.S. and Eskin, E. (2018) 'Population structure in genetic studies: Confounding factors and mixed models', *PLOS Genetics*. Edited by G.S. Barsh, 14(12), p. e1007309. Available at: <https://doi.org/10.1371/journal.pgen.1007309>.
- Thal, D.R. et al. (2002) 'Phases of A β -deposition in the human brain and its relevance for the development of Alzheimer's disease', *Neurology*, 58(12), pp. 1791-1800.
- Tierney, N. and Cook, D. (2023) 'Expanding Tidy Data Principles to Facilitate Missing Data Exploration, Visualization and Assessment of Imputations', *Journal of Statistical Software*, 105(7), pp. 1-31. Available at: <https://doi.org/10.18637/jss.v105.i07>.
- Tingley, D. et al. (2014) 'mediation: R Package for Causal Mediation Analysis', *Journal of Statistical Software*, 59(5), pp. 1-38. Available at: <https://doi.org/10.18637/jss.v059.i05>.

Trampush, J.W. et al. (2017) 'GWAS meta-analysis reveals novel loci and genetic correlates for general cognitive function: a report from the COGENT consortium', *Molecular Psychiatry*, 22(3), pp. 336–345. Available at: <https://doi.org/10.1038/mp.2016.244>.

Tu, T. and Ochoa, A. (2025) 'Genetic association meta-analysis is susceptible to confounding by between-study cryptic relatedness'. *Genetics*. Available at: <https://doi.org/10.1101/2025.05.10.653279>.

Tunbridge, E.M. et al. (2019) 'Which dopamine polymorphisms are functional? Systematic review and meta-analysis of COMT, DAT, DBH, DDC, DRD1-5, MAOA, MAOB, TH, VMAT1, and VMAT2', *Biological Psychiatry*, 86(8), pp. 608–620. Available at: <https://doi.org/10.1016/j.biopsych.2019.05.014>.

Tunbridge, E.M. et al. (2020) 'The role of catechol-O-methyltransferase in modulating human cognition', *Biological Psychiatry*, 88(2), pp. 74–83.

Turner, S. (2018) 'qqman: an R package for visualizing GWAS results using Q-Q and manhattan plots', *The Journal of Open Source Software* [Preprint]. Available at: <https://doi.org/10.21105/joss.00731>.

United Nations Department of Economic and Social Affairs, Population Division (2022) World Population Prospects 2022: Summary of Results. UN DESA/POP/2022/TR/NO. 3. New York: United Nations. Available at: www.unpopulation.org.

Van Dyck, C.H. et al. (2008) 'Striatal dopamine transporters correlate with simple reaction time in elderly subjects', *Neurobiology of Aging*, 29(8), pp. 1237–1246. Available at: <https://doi.org/10.1016/j.neurobiolaging.2007.02.012>.

Verhaeghen, P. and Salthouse, T.A. (1997) 'Meta-analyses of age-cognition relations in adulthood: estimates of linear and nonlinear age effects and structural models', *Psychological Bulletin*, 122(3), pp. 231–249. Available at: <https://doi.org/10.1037/0033-2909.122.3.231>.

Vriend, C. et al. (2020) 'Processing speed is related to striatal dopamine transporter availability in Parkinson's disease', *NeuroImage: Clinical*, 26, p. 102257. Available at: <https://doi.org/10.1016/j.nicl.2020.102257>.

Walker, K.A., Power, M.C. and Gottesman, R.F. (2017) 'Defining the Relationship Between Hypertension, Cognitive Decline, and Dementia: a Review', *Current hypertension reports*, 19(3), p. 24. Available at: <https://doi.org/10.1007/s11906-017-0724-3>.

Wennberg, A.M. et al. (2019) 'The influence of tau, amyloid, alpha-synuclein, TDP-43, and vascular pathology in clinically normal elderly individuals', *Neurobiology of Aging*, 77, pp. 26–36. Available at:
<https://doi.org/10.1016/j.neurobiolaging.2019.01.008>.

Woo, N.H. and Lu, B. (2009) 'BDNF in Synaptic Plasticity and Memory', in Encyclopedia of Neuroscience. Elsevier, pp. 135–143. Available at:
<https://doi.org/10.1016/B978-008045046-9.00829-9>.

Xu, H. and Yang, F. (2022) 'The interplay of dopamine metabolism abnormalities and mitochondrial defects in the pathogenesis of schizophrenia', *Transl Psychiatry*, 12, p. 464. Available at: <https://doi.org/10.1038/s41398-022-02233-0>.

Yang, T. et al. (2020) 'The Role of BDNF on Neural Plasticity in Depression', *Frontiers in Cellular Neuroscience*, 14, p. 82. Available at: <https://doi.org/10.3389/fncel.2020.00082>.

Zeggini, E. and Morris, A. (eds) (2015) Assessing Rare Variation in Complex Traits: Design and Analysis of Genetic Studies. New York, NY: Springer New York. Available at: <https://doi.org/10.1007/978-1-4939-2824-8>.

Zhang, K. et al. (2010) 'Human tyrosine hydroxylase natural genetic variation: delineation of functional transcriptional control motifs disrupted in the proximal promoter', *Circulation: Cardiovascular Genetics*, 3(2), pp. 187–198. Available at: <https://doi.org/10.1161/CIRCGENETICS.109.904813>.

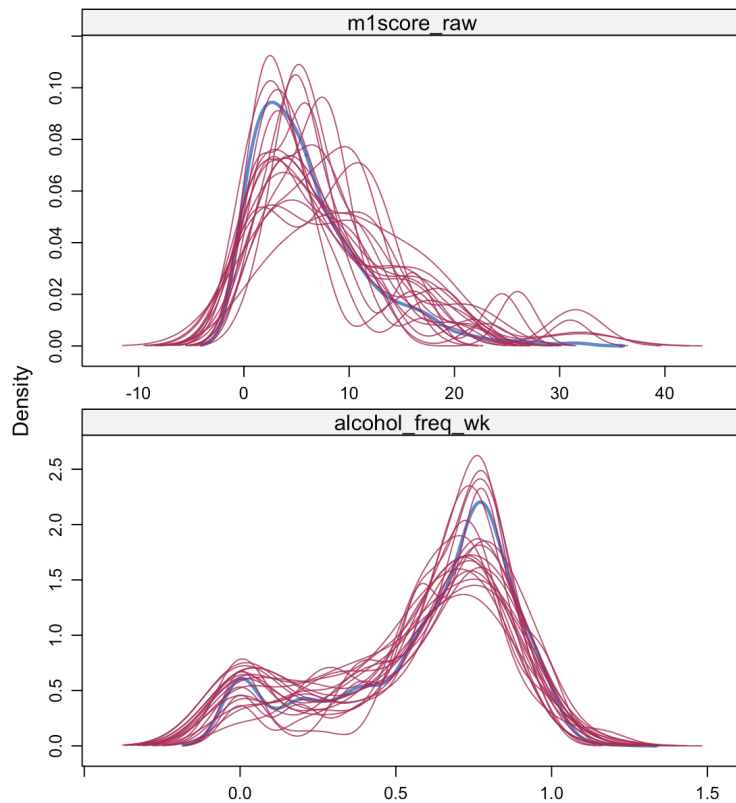
8. Appendices

Appendix A1. SNP Retention by Candidate Gene.

Gene	SNPs_pre	SNPs_post	Indiv_pre	Indiv_post	LDpruned	HWE_fail
COMT	387	237	1563	1479	353	0
DRD2	147	119	1563	1464	128	0
DRD3	172	107	1563	1534	155	0
DAT1	104	104	1563	1500	88	0
DBH	88	49	1563	1444	73	0
PPP1R1B	17	8	1563	1532	14	0
DDC	439	325	1563	1493	423	0
DRD1	6	6	1563	1547	3	0
TH	2	2	1563	1563	0	0
DRD5	1	0	1563	1559	0	0

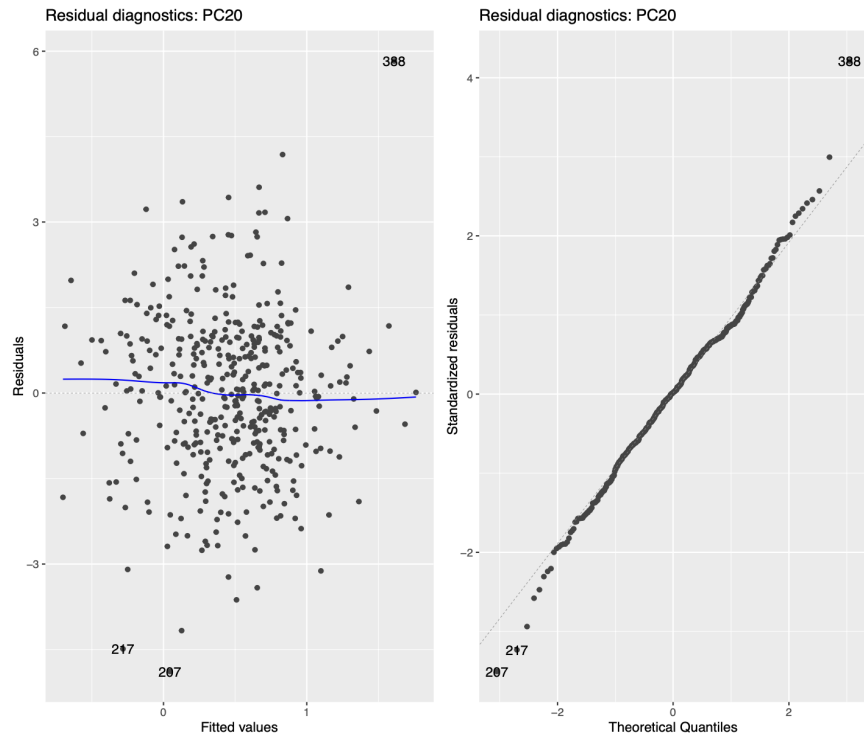
Summary of SNP and individual counts for each gene throughout the quality control pipeline. SNPs_pre/post and Indiv_pre/post show the counts before and after filtering, respectively. LDpruned indicates variants removed for linkage disequilibrium, and HWE_fail indicates variants that failed Hardy-Weinberg equilibrium tests.

Appendix A2. Density plots comparing observed and imputed values for baseline cognitive score and alcohol-use frequency.



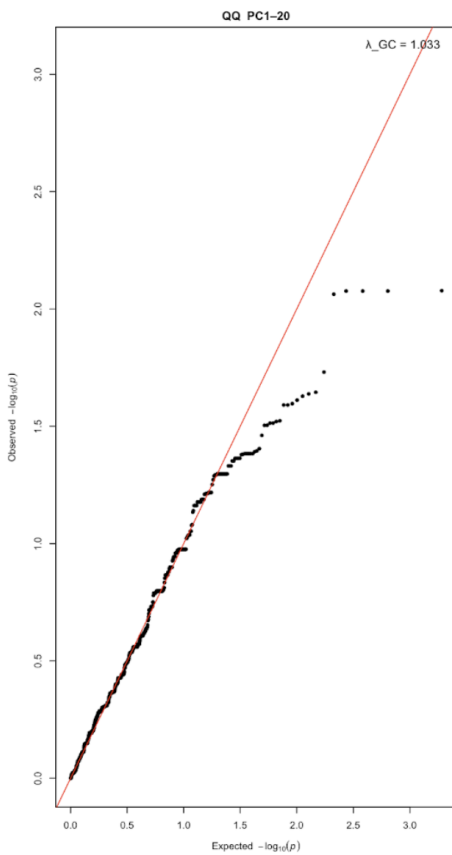
Density plots comparing the distributions of original observed values (blue line) with 20 imputed datasets (red lines) for the baseline BDI mood score and self-reported alcohol-use frequency.

Appendix A3. Preliminary regression model diagnostics for covariate assessment.



Diagnostic plots for the primary regression model (processing speed slope with PC1-20 adjustment). Left: Residuals versus fitted values plot to assess homoscedasticity. Right: Normal quantile-quantile (Q-Q) plot to assess the normality of model residuals.

Appendix A4. QQ plot of SNP association p-values for processing-speed slope (PC1-20 model).



The plot compares the distribution of observed p -values (black points) from the processing speed slope analysis against the expected distribution under the null hypothesis (red line).

Appendix A5. Top 10 SNP-level associations for secondary cognitive domains (Cognitive Slopes).

SECONDARY: Fluid Reasoning SLOPES (Decline Rate)

Chr	SNP ID	Gene	Effect			SE	L95	U95	Raw P-value	P_bonf	q (FDR)	
			Allele	A2	EAF							
5	rs12518222	DRD1	T	C	0.144	0.3508	0.1132	0.1289	0.5727	0.002	1	0.84
5	rs5326	DRD1	T	C	0.144	0.3508	0.1132	0.1289	0.5727	0.002	1	0.84
17	rs1495099	PPP1R1B	C	G	0.272	-0.2390	0.0878	-0.4111	-0.0669	0.007	1	0.84
9	rs1611123	DBH	T	C	0.436	-0.3311	0.1326	-0.5910	-0.0712	0.013	1	0.84
5	rs4867798	DRD1	C	T	0.300	0.2036	0.0871	0.0329	0.3743	0.020	1	0.84
9	rs2519152	DBH	C	T	0.436	-0.2834	0.1354	-0.5488	-0.0180	0.037	1	0.84
17	rs3794712	PPP1R1B	A	C	0.176	-0.2045	0.1018	-0.4040	-0.0050	0.045	1	0.84
3	rs76126170	DRD3	T	C	0.079	0.3680	0.1850	0.0054	0.7306	0.047	1	0.84
3	rs75982648	DRD3	A	G	0.079	0.3680	0.1850	0.0054	0.7306	0.047	1	0.84
3	rs6787134	DRD3	G	T	0.132	0.7725	0.3947	-0.0011	1.5461	0.051	1	0.84

Abbreviations: Chr, chromosome; A2, other allele; EAF, effect allele frequency; β (SD), effect size in standard deviation units; SE, standard error; L95/U95, 95% confidence interval; P_bonf, Bonferroni-corrected p-value; q(FDR), false discovery rate.

SECONDARY: Episodic Memory SLOPES (Decline Rate)

Chr	SNP ID	Gene	Effect			SE	L95	U95	Raw P-value	P_bonf	q (FDR)	
			Allele	A2	EAF							
22	rs756661	COMT	G	A	0.465	-0.3915	0.1468	-0.6792	-0.1038	0.008	1	0.846
22	rs885987	COMT	A	G	0.464	-0.3875	0.1473	-0.6762	-0.0988	0.009	1	0.846
11	rs7948028	DRD2	C	A	0.385	0.2818	0.1078	0.0705	0.4931	0.009	1	0.846
11	rs11601054	DRD2	A	G	0.385	0.2818	0.1078	0.0705	0.4931	0.009	1	0.846
11	rs61902787	DRD2	A	C	0.385	0.2818	0.1078	0.0705	0.4931	0.009	1	0.846
11	rs61902807	DRD2	C	T	0.385	0.2818	0.1078	0.0705	0.4931	0.009	1	0.846
11	rs4630328	DRD2	A	G	0.383	0.2837	0.1086	0.0708	0.4966	0.009	1	0.846
22	rs5993864	COMT	C	T	0.469	-0.3752	0.1444	-0.6582	-0.0922	0.010	1	0.846
22	rs737862	COMT	G	C	0.469	-0.3812	0.1486	-0.6725	-0.0899	0.011	1	0.846
11	rs4337071	DRD2	T	C	0.384	0.2741	0.1081	0.0622	0.4860	0.012	1	0.846

Abbreviations: Chr, chromosome; A2, other allele; EAF, effect allele frequency; β (SD), effect size in standard deviation units; SE, standard error; L95/U95, 95% confidence interval; P_bonf, Bonferroni-corrected p-value; q(FDR), false discovery rate.

SECONDARY: Vocabulary SLOPES (Decline Rate)

Chr	SNP ID	Gene	Effect Allele	A2	EAF	β (SD)	SE	L95	U95	Raw P-value	P_bonf	q (FDR)
9	rs3025382	DBH	A	G	0.145	0.6617	0.2202	0.2301	1.0933	0.003	1	0.535
7	rs10277662	DDC	T	C	0.207	1.3500	0.4603	0.4478	2.2522	0.004	1	0.535
7	rs9942686	DDC	A	G	0.207	1.3500	0.4603	0.4478	2.2522	0.004	1	0.535
7	rs11575320	DDC	T	C	0.207	1.3500	0.4603	0.4478	2.2522	0.004	1	0.535
7	rs3779078	DDC	T	C	0.207	1.3500	0.4603	0.4478	2.2522	0.004	1	0.535
7	rs3807556	DDC	A	G	0.206	1.3500	0.4617	0.4451	2.2549	0.004	1	0.535
7	rs4515495	DDC	T	A	0.189	-0.4565	0.1633	-0.7766	-0.1364	0.005	1	0.535
7	rs12671474	DDC	A	C	0.207	1.3170	0.4726	0.3907	2.2433	0.006	1	0.535
7	rs10267323	DDC	G	A	0.207	1.3170	0.4726	0.3907	2.2433	0.006	1	0.535
7	rs10271341	DDC	G	T	0.207	1.3170	0.4726	0.3907	2.2433	0.006	1	0.535

Abbreviations: Chr, chromosome; A2, other allele; EAF, effect allele frequency; β (SD), effect size in standard deviation units; SE, standard error; L95/U95, 95% confidence interval; P_bonf, Bonferroni-corrected p-value; q(FDR), false discovery rate.

Top 10 SNP associations for the decline slopes of fluid reasoning, episodic memory, and vocabulary. All models are fully adjusted (PC1–20).

Appendix A6. Top 10 SNP-level associations for secondary cognitive domains (Cognitive Intercepts).

SECONDARY: Fluid Reasoning INTERCEPTS (Performance at Age 70)

Chr	SNP ID	Gene	Effect Allele	A2	EAF	β (SD)	SE	L95	U95	Raw P-value	P_bonf	q (FDR)
9	rs2097629	DBH	G	A	0.371	0.2126	0.0787	0.0583	0.3669	0.007	1	0.758
9	rs2097628	DBH	G	A	0.372	0.2033	0.0784	0.0496	0.3570	0.010	1	0.758
9	rs10761412	DBH	C	T	0.378	0.2042	0.0792	0.0490	0.3594	0.010	1	0.758
7	rs11765748	DDC	T	A	0.456	0.5676	0.2337	0.1095	1.0257	0.016	1	0.758
7	rs10499694	DDC	A	G	0.457	0.5651	0.2328	0.1088	1.0214	0.016	1	0.758
3	rs6795188	DRD3	G	A	0.068	0.4528	0.1937	0.0731	0.8325	0.020	1	0.758
9	rs77905	DBH	A	G	0.486	-0.1715	0.0762	-0.3209	-0.0221	0.025	1	0.758
11	rs10789943	DRD2	A	G	0.141	0.2454	0.1093	0.0312	0.4596	0.025	1	0.758
22	rs5748475	COMT	T	C	0.489	-0.5287	0.2401	-0.9993	-0.0581	0.028	1	0.758
22	rs5748477	COMT	C	G	0.489	-0.5287	0.2401	-0.9993	-0.0581	0.028	1	0.758

Abbreviations: Chr, chromosome; A2, other allele; EAF, effect allele frequency; β (SD), effect size in standard deviation units; SE, standard error; L95/U95, 95% confidence interval; P_bonf, Bonferroni-corrected p-value; q(FDR), false discovery rate.

SECONDARY: Episodic Memory INTERCEPTS (Performance at Age 70)

Chr	SNP ID	Gene	Effect Allele	A2	EAF	β (SD)	SE	L95	U95	Raw P-value	P_bonf	q (FDR)
7	rs11575429	DDC	G	C	0.118	-1.5260	0.5497	-2.6034	-0.4486	0.006	1	0.842
7	rs2329371	DDC	A	G	0.212	0.8312	0.3676	0.1107	1.5517	0.024	1	0.842
22	rs4646316	COMT	T	C	0.247	-0.2419	0.1073	-0.4522	-0.0316	0.025	1	0.842
11	rs11214607	DRD2	G	T	0.168	0.7716	0.3490	0.0876	1.4556	0.028	1	0.842
11	rs4648319	DRD2	A	G	0.168	0.7716	0.3490	0.0876	1.4556	0.028	1	0.842
3	rs62267152	DRD3	C	G	0.210	-0.6739	0.3248	-1.3105	-0.0373	0.039	1	0.842
3	rs7631639	DRD3	G	C	0.315	-0.7282	0.3578	-1.4295	-0.0269	0.043	1	0.842
3	rs77489111	DRD3	T	C	0.064	1.8170	0.9090	0.0354	3.5986	0.046	1	0.842
3	rs111522445	DRD3	T	C	0.064	1.8170	0.9090	0.0354	3.5986	0.046	1	0.842
3	rs112718054	DRD3	G	T	0.064	1.8170	0.9090	0.0354	3.5986	0.046	1	0.842

Abbreviations: Chr, chromosome; A2, other allele; EAF, effect allele frequency; β (SD), effect size in standard deviation units; SE, standard error; L95/U95, 95% confidence interval; P_bonf, Bonferroni-corrected p-value; q(FDR), false discovery rate.

SECONDARY: Vocabulary INTERCEPTS (Performance at Age 70)

Chr	SNP ID	Gene	Effect Allele	A2	EAF	β (SD)	SE	L95	U95	Raw P-value	P_bonf	q (FDR)
11	rs10789943	DRD2	A	G	0.141	0.2743	0.1015	0.0754	0.4732	0.007	1	0.747
11	rs7122454	DRD2	C	G	0.135	0.2658	0.1032	0.0635	0.4681	0.010	1	0.747
11	rs11214611	DRD2	G	A	0.135	0.2658	0.1032	0.0635	0.4681	0.010	1	0.747
11	rs4648317	DRD2	A	G	0.135	0.2658	0.1032	0.0635	0.4681	0.010	1	0.747
11	rs10891551	DRD2	A	G	0.135	0.2658	0.1032	0.0635	0.4681	0.010	1	0.747
7	rs11765748	DDC	T	A	0.456	0.5569	0.2165	0.1326	0.9812	0.010	1	0.747
11	rs10891550	DRD2	C	G	0.137	0.2628	0.1031	0.0607	0.4649	0.011	1	0.747
7	rs10499694	DDC	A	G	0.457	0.5495	0.2158	0.1265	0.9725	0.011	1	0.747
11	rs7117915	DRD2	A	G	0.136	0.2595	0.1033	0.0570	0.4620	0.012	1	0.747
11	rs4350392	DRD2	A	C	0.136	0.2595	0.1033	0.0570	0.4620	0.012	1	0.747

Abbreviations: Chr, chromosome; A2, other allele; EAF, effect allele frequency; β (SD), effect size in standard deviation units; SE, standard error; L95/U95, 95% confidence interval; P_bonf, Bonferroni-corrected p-value; q(FDR), false discovery rate.

Top 10 SNP associations for performance intercepts (at age 70) in fluid reasoning, episodic memory, and vocabulary. All models are fully adjusted (PC1–20).

Appendix A7. Gene-based association results for secondary cognitive domains (Cognitive Slopes).

Fluid Intelligence Slopes (SECONDARY)

Dopamine genes (N=434)					
Gene	N SNPs	Z-stat	P-value	P_bonf	q (FDR)
DRD1	5	1.830	0.034	0.269	0.198
PPP1R1B	8	1.649	0.050	0.397	0.198
DBH	49	0.522	0.301	1.000	0.669
DRD3	105	0.083	0.467	1.000	0.669
COMT	43	-0.032	0.513	1.000	0.669
SLC6A3	104	-0.135	0.554	1.000	0.669
DRD2	117	-0.215	0.585	1.000	0.669
DDC	323	-0.439	0.670	1.000	0.670

Abbreviations: N SNPs, number of variants in gene; Z-stat, MAGMA test statistic; P_bonf, Bonferroni-corrected p-value; q(FDR), false discovery rate.

Memory Slopes (SECONDARY)

Dopamine genes (N=434)					
Gene	N SNPs	Z-stat	P-value	P_bonf	q (FDR)
DRD2	117	1.586	0.056	0.451	0.451
SLC6A3	104	0.218	0.414	1.000	0.742
DBH	49	0.159	0.437	1.000	0.742
DRD3	105	0.036	0.486	1.000	0.742
PPP1R1B	8	-0.202	0.580	1.000	0.742
DDC	323	-0.359	0.640	1.000	0.742
COMT	43	-0.384	0.649	1.000	0.742
DRD1	5	-1.238	0.892	1.000	0.892

Abbreviations: N SNPs, number of variants in gene; Z-stat, MAGMA test statistic; P_bonf, Bonferroni-corrected p-value; q(FDR), false discovery rate.

Vocabulary Slopes (SECONDARY)

Dopamine genes (N=434)

Gene	N SNPs	Z-stat	P-value	P_bonf	q (FDR)
PPP1R1B	8	1.646	0.050	0.399	0.399
DDC	323	0.746	0.228	1.000	0.706
DRD3	105	0.629	0.265	1.000	0.706
DRD1	5	0.277	0.391	1.000	0.710
COMT	43	-0.169	0.567	1.000	0.710
DBH	49	-0.296	0.616	1.000	0.710
DRD2	117	-0.308	0.621	1.000	0.710
SLC6A3	104	-1.246	0.894	1.000	0.894

Abbreviations: N SNPs, number of variants in gene; Z-stat, MAGMA test statistic; P_bonf, Bonferroni-corrected p-value; q(FDR), false discovery rate.

Gene-level association results from MAGMA analysis for fluid intelligence, episodic memory, and visuospatial memory slopes. Each table shows results for eight dopamine pathway genes, ranked by p-value within each domain.

Appendix A8. Gene-based association results for secondary cognitive domains (Cognitive Intercepts).

Fluid Intelligence Intercepts (SECONDARY)

Dopamine genes (N=434)

Gene	N SNPs	Z-stat	P-value	P_bonf	q (FDR)
DRD3	105	0.966	0.167	1	0.582
PPP1R1B	8	0.514	0.304	1	0.582
COMT	43	0.509	0.305	1	0.582
DRD2	117	0.439	0.330	1	0.582
DBH	49	0.349	0.364	1	0.582
DDC	323	-0.049	0.519	1	0.693
DRD1	5	-0.645	0.741	1	0.846
SLC6A3	104	-1.762	0.961	1	0.961

Abbreviations: N SNPs, number of variants in gene; Z-stat, MAGMA test statistic; P_bonf, Bonferroni-corrected p-value; q(FDR), false discovery rate.

Memory Intercepts (SECONDARY)

Dopamine genes (N=434)

Gene	N SNPs	Z-stat	P-value	P_bonf	q (FDR)
DRD3	105	1.080	0.140	1	0.606
DRD2	117	0.481	0.315	1	0.606
COMT	43	0.291	0.386	1	0.606
PPP1R1B	8	0.168	0.433	1	0.606
SLC6A3	104	0.145	0.442	1	0.606
DDC	323	-0.120	0.548	1	0.606
DBH	49	-0.211	0.584	1	0.606
DRD1	5	-0.269	0.606	1	0.606

Abbreviations: N SNPs, number of variants in gene; Z-stat, MAGMA test statistic; P_bonf, Bonferroni-corrected p-value; q(FDR), false discovery rate.

Vocabulary Intercepts (SECONDARY)

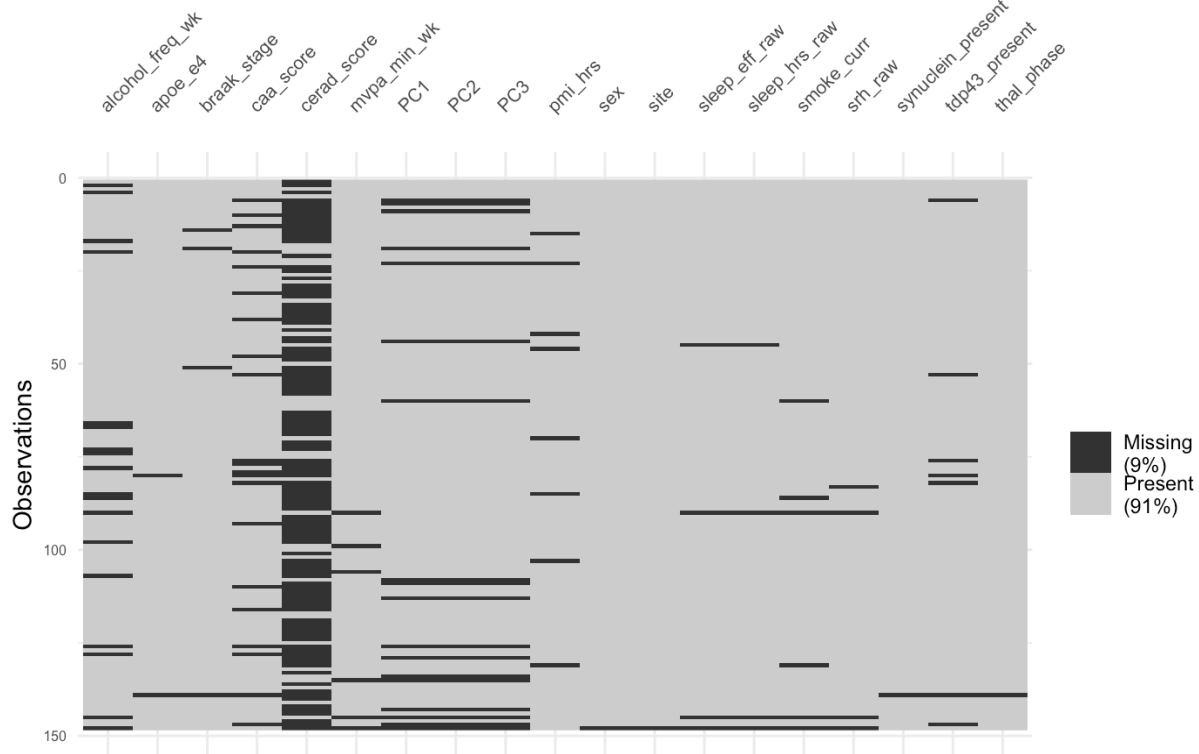
Dopamine genes (N=434)					
Gene	N SNPs	Z-stat	P-value	P_bonf	q (FDR)
DRD3	105	1.264	0.103	0.825	0.709
PPP1R1B	8	0.398	0.345	1.000	0.709
DRD2	117	0.323	0.373	1.000	0.709
DBH	49	-0.096	0.538	1.000	0.709
SLC6A3	104	-0.202	0.580	1.000	0.709
DDC	323	-0.370	0.644	1.000	0.709
COMT	43	-0.417	0.662	1.000	0.709
DRD1	5	-0.552	0.709	1.000	0.709

Abbreviations: N SNPs, number of variants in gene; Z-stat, MAGMA test statistic; P_bonf, Bonferroni-corrected p-value; q(FDR), false discovery rate.

Gene-level association results from MAGMA analysis for fluid intelligence, episodic memory, and visuospatial memory intercepts. Each table shows results for eight dopamine pathway genes, ranked by p-value within each domain.

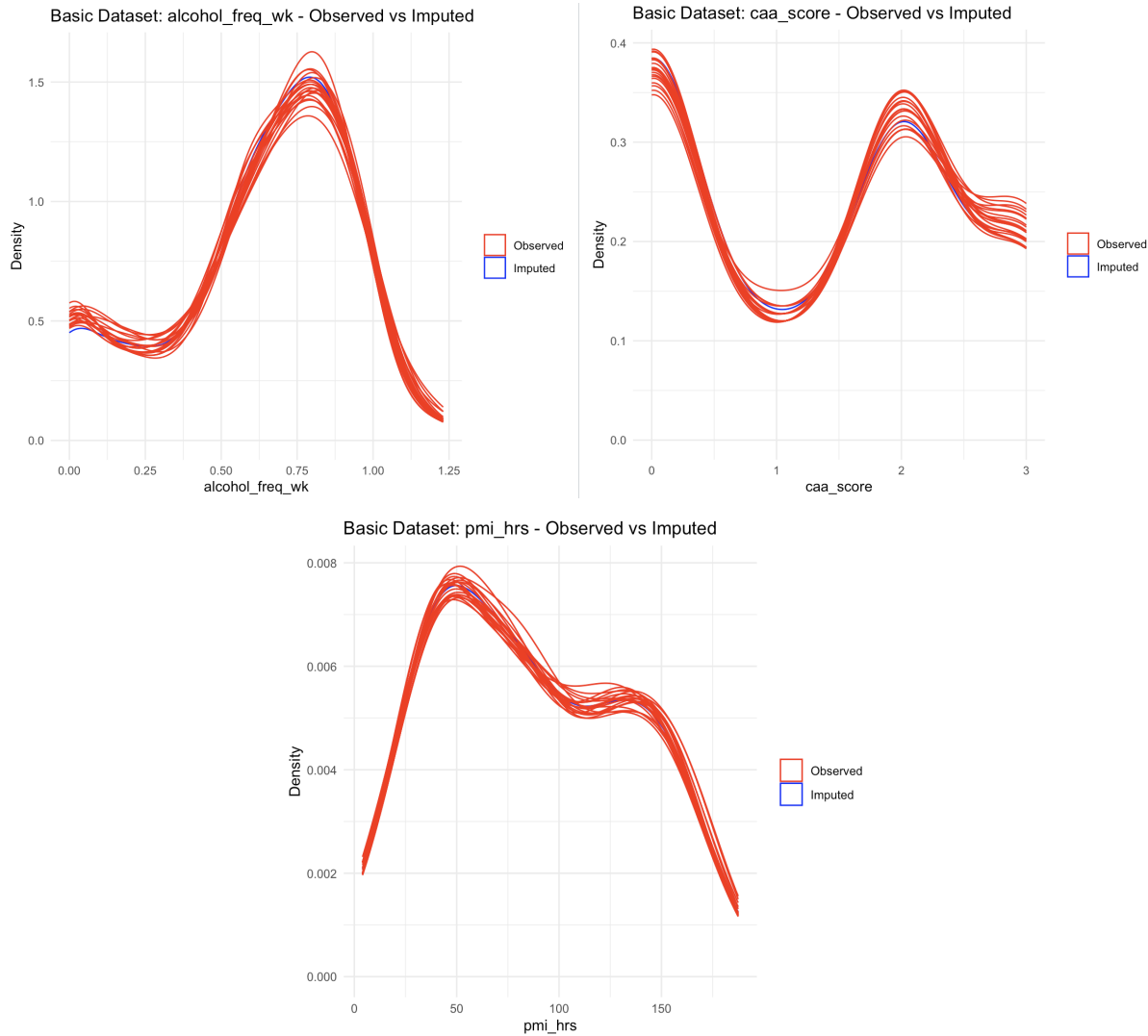
Appendix A9. Missing data patterns for basic covariates and neuropathology variables (n=148).

Missing Data: Basic Covariates + Neuropathology



Heat-map illustrating the pattern of missing data across all variables in the initial neuropathology subset (n=148). Black bars indicate missing values; gray indicates observed data.

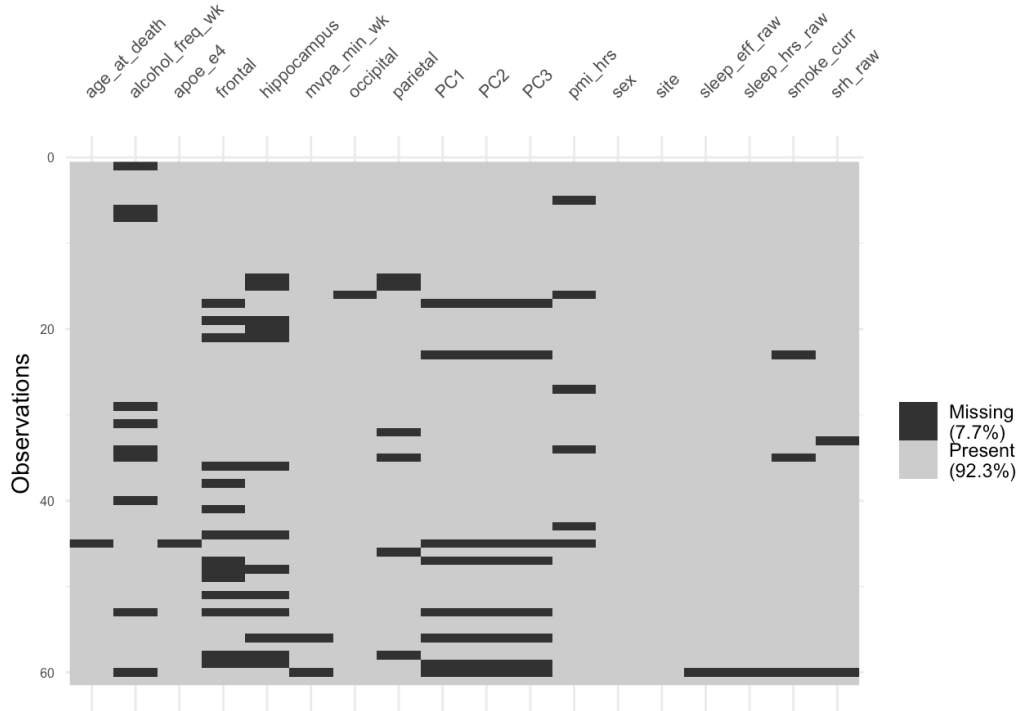
Appendix A10. Multiple imputation diagnostic plots for neuropathology variables.



Density plots comparing the distributions of original observed values (blue line) with 20 imputed datasets (red lines) for alcohol consumption frequency, CAA score, and post-mortem interval.

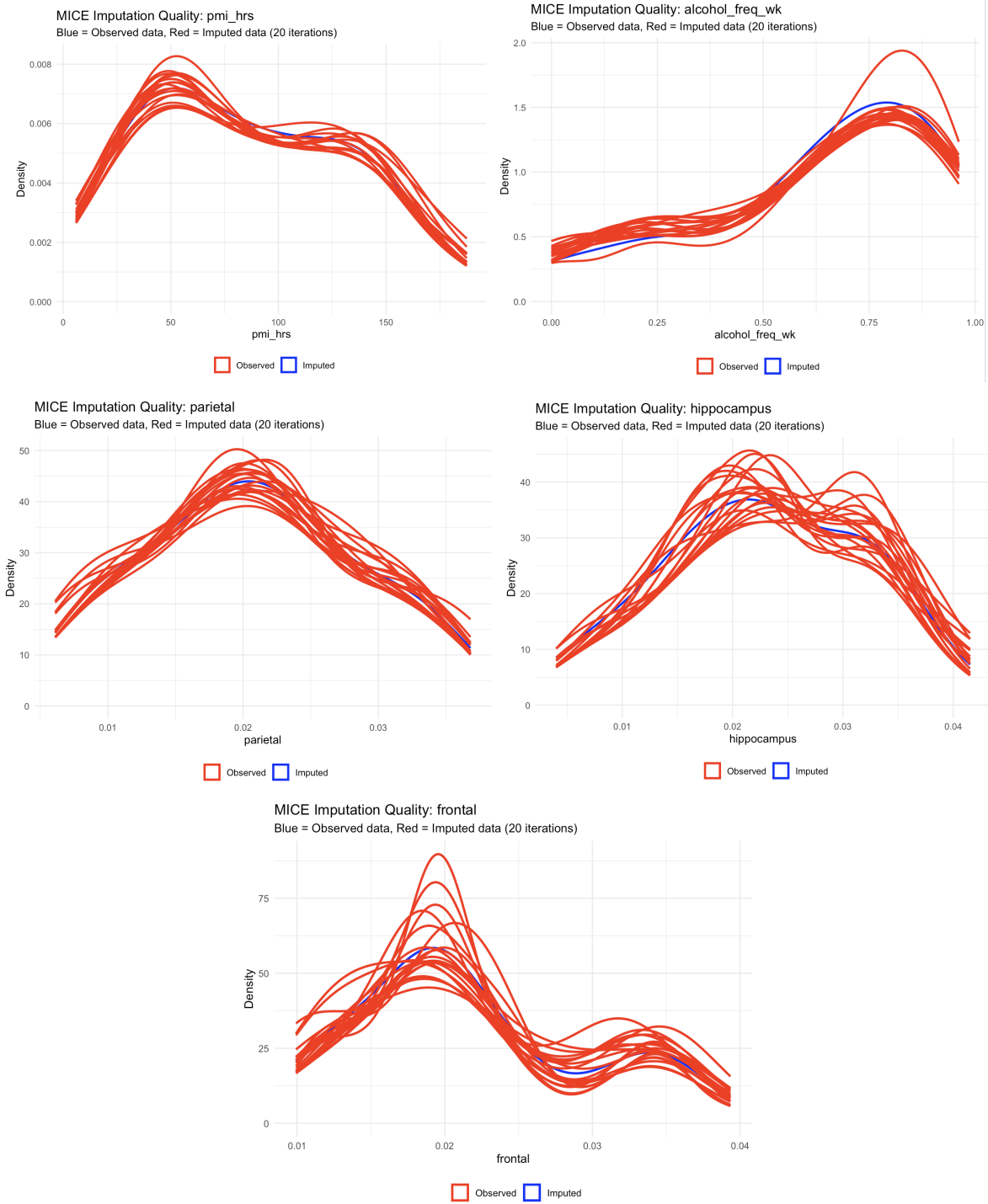
Appendix A11. Missing data patterns for synaptic density analysis covariates (n=61).

Updated Missing Data: Synaptic Density + Complete Covariates



Heat-map illustrating the pattern of missing data across all variables in the initial synaptic density subset (n=61). Black bars indicate missing values; gray indicates observed data.

Appendix A12. Multiple imputation diagnostic plots for synaptic density variables.



Density plots comparing the distributions of original observed values (blue line) with 20 imputed datasets (red lines) for post-mortem interval, alcohol frequency, and synaptic density measures in three cortical regions.

